Available online at www.sciencedirect.com
SCIENCE DIRECT®
Ecological Modelling 193 (2006) 412–436
ECOLOGICAL MODELLING
www.elsevier.com/locate/ecolmodel

A numerical simulation of the role of zooplankton in C, N and P cycling in Lake Kinneret, Israel

Louise C. Bruce [a,*], David Hamilton [b], Jörg Imberger [a], Gideon Gal [c], Moshe Gophen [d], Tamar Zohary [c], K. David Hambright [e]

[a] *Centre for Water Research, University of Western Australia, 35 Stirling Highway, Crawley, WA 6009, Australia*
[b] *Department of Biological Sciences, The University of Waikato, Private Bag 3105, Hamilton, New Zealand*
[c] *Y. Allon Kinneret Limnological Laboratory, IOLR, P.O. Box 447, Migdal 14950, Israel*
[d] *Limnology and Ecology of Wetlands and Freshwater, MIGAL Galilee Technology Centre, Southern Industrial Zone, P.O. Box 831, Kiryat-Shmona 11016, Israel*
[e] *University of Oklahoma Biological Station and Department of Zoology, HC-71, Box 205, Kingston, OK 73439, USA*

Received 6 February 2005; received in revised form 30 August 2005; accepted 7 September 2005
Available online 10 November 2005

Abstract

We quantify the role of zooplankton in nutrient cycles in Lake Kinneret, Israel, using field data and a numerical model. A coupled ecological and hydrodynamic model (Dynamic Reservoir Model (DYRESM)–Computational Aquatic Ecosystem Dynamics Model (CAEDYM)) was validated with an extensive field data set to simulate the seasonal dynamics of nutrients, three phytoplankton groups and three zooplankton groups. Parameterization of the model was conducted using field, experimental and literature studies. Sensitivity of simulated output was tested over the full parameter space and established that the most sensitive parameters were related to zooplankton grazing rates, temperature responses and food limitation. The simulated results predict that, on average, 51% of the carbon from phytoplankton photosynthesis is consumed by zooplankton. Excretion of dissolved nutrients by zooplankton accounts for 3–46 and 5–58% of phytoplankton uptake of phosphorus and nitrogen, respectively. Comparison of nutrient fluxes attributable to zooplankton with nutrient loads from inflows and release from bottom sediments shows that the relative contribution by zooplankton to inorganic nutrients in the photic zone varies seasonally in response to the annual hydrodynamic cycle of stratification and mixing. As a percent of total dissolved organic sources relative contributions by zooplankton excretion are highest (62%) during periods of stratification and when inflow nutrient loads are low, and lowest (2%) during the breakdown of stratification and when inflow loads are high. The results illustrate the potential of a lake ecosystem model to extract useful process information to complement field data collection and address questions related to the role of zooplankton in nutrient cycles.

Keywords: Zooplankton; Nutrient cycling; Numerical model; Lake Kinneret

* Corresponding author.

0304-3800/$ – see front matter © 2005 Elsevier B.V. All rights reserved.
doi:10.1016/j.ecolmodel.2005.09.008

1. Introduction

Zooplankton play an important role in lake dynamics, as grazers that control algal and bacterial populations, as a food source for higher trophic levels and in the excretion of dissolved nutrients. Thus, understanding their role in the distribution and flux of nutrients in aquatic systems is critical for effective lake management. Zooplankton grazing on phytoplankton can transfer more than 50% of carbon fixed by primary production to higher trophic levels (Hart et al., 2000; Laws et al., 1988; Scavia, 1980). Zooplankton excretion strongly influences trophic dynamics in freshwater ecosystems by contributing inorganic N and P for primary and bacterial production (Gilbert, 1998; Lehman, 1980; Sterner, 1986; Vanni, 2002; Wen and Peters, 1994). Estimates of the fraction of N and P regenerated by zooplankton and then utilised by phytoplankton range from 14 to 50% (Hudson and Taylor, 1996; Hudson et al., 1999; Urabe et al., 1995). The factors controlling this fraction include temperature, zooplankton and phytoplankton biomass and species composition, internal nutrient ratios and mixing regimes. Because these factors interact dynamically, it has been difficult to quantify the role of zooplankton in nutrient cycling.

Models have previously been used to evaluate different aspects of zooplankton dynamics in lakes (Carpenter and Kitchell, 1993; Chen et al., 2002; Cole et al., 2002; Håkanson and Boulion, 2003; Hongping and Jianyi, 2002; Ji et al., 2005; Krivtsov et al., 2001; Lunte and Leucke, 1990; Rukhovets et al., 2003; Scavia et al., 1988), reservoirs (Mehner, 2000; Osidele and Beck, 2004; Romero et al., 2004), fjords (Ross et al., 1994), estuaries (Griffin et al., 2000; Robson and Hamilton, 2004), lagoons (Lin et al., 1999) and in the marine environment (Carlotti and Günther, 1996; Laws et al., 1988). The models range in complexity from simple mass balances to highly parameterized simulation tools that include hydrodynamic processes (Carlotti and Günther, 1996; Robson and Hamilton, 2004; Ross et al., 1994). Some models simulate nutrient fluxes between trophic levels and provide valuable insights into the relative importance of zooplankton in nutrient cycles (Urabe et al., 1995). These models may also yield more detailed temporal and spatial information on nutrient fluxes between different trophic levels in a lake than is often possible with field or laboratory data. Specifically, models can be used to predict how the fluxes change in response to environmental factors or lake management strategies.

Lake Kinneret has been studied intensely both in situ and experimentally (Hambright et al., 1994; Serruya, 1978; Yacobi et al., 1993; Zohary et al., 1994). The lake supplies approximately 30% of Israel's drinking water, a fact that has motivated an extensive water quality and ecological monitoring program as well as a major subsidized fishing effort to rid the lake of planktivorous sardines in the hope of fostering the existing zooplankton population (Blumenshine and Hambright, 2003). The monitoring program has included routine sampling of various levels of the lake food web, including zooplankton and phytoplankton, water column and tributary chemical and physical parameters, and meteorological data.

In this study, we have applied a coupled ecological and hydrodynamic model (DYRESM–CAEDYM) to the Lake Kinneret data set to simulate the seasonal dynamics of nutrients, three phytoplankton groups and three zooplankton groups. The true uniqueness of this study lies in the mechanistic approach to model structure, low vertical resolution of the physical driver requiring only external forcing, sub-daily time steps, multi-nutrient focus, division of both phytoplankton and zooplankton into functional groups and the application against an extensive data set. Although simple mass balance box models such as Hart et al. (2000) can be useful in determining lake wide patterns, the processes represented in CAEDYM allowed us to focus on specific mechanisms responsible for the determination of important lake phenomenon. The fully mechanistic structure of DYRESM means that no calibration is required (Yeates and Imberger, 2004); the other advantage of using DYRESM is the vertical resolution so that processes such as sediment release and particulate settling are fully represented rather than forced as inputs such as in Osidele and Beck (2004). In addition, a sub-daily time step in both the ecological model and hydrodynamic driver enables resolution of photosynthetic processes so that seasonal trends can be more accurately resolved rather than the use of daily or weekly time steps such as those used by Håkanson and Boulion (2003). Many ecosystem models are developed based on a single limiting nutrient (Ji et al., 2005). CAEDYM on the other hand explicitly models the inorganic, organic, phytoplankton and zooplankton

components of carbon, nitrogen and phosphorus. This approach is crucial in lake such as Lake Kinneret where limitation can switch between nitrogen and phosphorus depending on the season. Although some ecological models divide phytoplankton into functional groups, most treat zooplankton as a single entity (Hongping and Jianyi, 2002; Krivtsov et al., 2001; Rukhovets et al., 2003). By including three phytoplankton and three zooplankton groups in the model, CAEDYM can be used to determine how the role of zooplankton changes as a function of changes in seasonal dominance between the main zooplankton groups. Finally, aquatic ecosystem models are often applied to lakes where data are scarce so that rigorous calibration and validation of models is difficult (Håkanson and Boulion, 2003; Osidele and Beck, 2004). The main advantage of the application of the model to such an extensive data set enabled us to test both the choice of parameters and model processes over a 4-year period. Although the application of some aquatic ecosystem models includes one or more of the attributes of DYRESM–CAEDYM described above, the contribution of our study is the inclusion of all together with a rigorous calibration and validation.

The objective of the present study was to investigate the role of zooplankton in the cycling of C, N and P between trophic levels in Lake Kinneret. After validating the coupled DYRESM–CAEDYM model against a comprehensive data set, we used the model to quantitatively examine how zooplankton biomass, secondary production and fluxes between trophic levels may be affected by seasonal changes in hydrodynamic mixing regimes. In addition, a sensitivity analysis was conducted to evaluate the relative importance of key parameters on model simulation results. The effect of zooplankton grazing and excretion on the availability of nutrients was estimated with the calibrated numerical model and compared to external sources from inflows and internal sources from sediment release.

2. Study site

Lake Kinneret (32°48′N, 35°37′E) is a warm-monomictic freshwater lake with maximum depth 43 m, mean depth 25 m and surface area approximately 170 km^2 (Fig. 1). The lake is vertically mixed in winter (December–February) and thermal stratification sets up in spring, persisting for 7–8 months. Temperature in the surface layer typically ranges from 15–17 °C in winter to 26–30 °C in summer (Hambright et al., 1994).

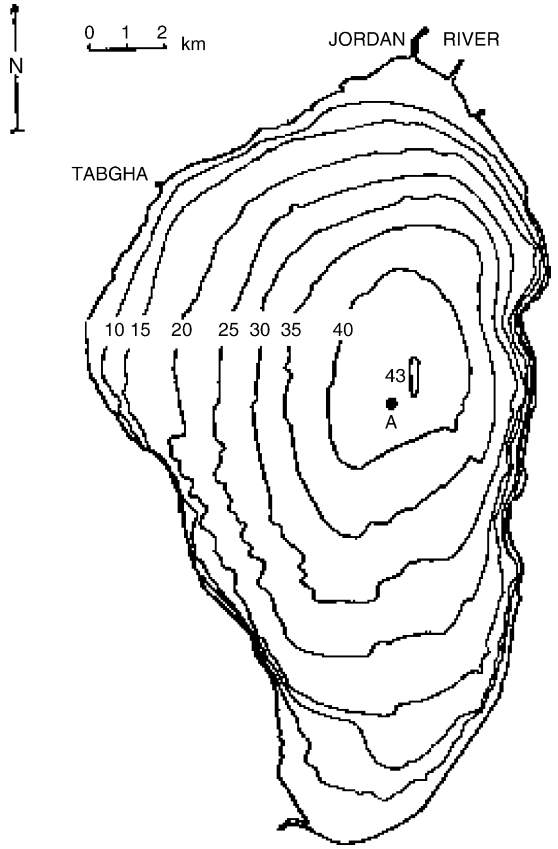

Fig. 1. Map of Lake Kinneret showing location of the main sampling station A and Jordan River inflow. Depth contours are in meters.

The phytoplankton assemblage of Lake Kinneret is generally dominated in winter–spring by the dinoflagellate *Peridinium gatunense*, in summer–autumn by a diverse assemblage of nanoplankton, mostly chlorophytes, and since the mid-1990s also by filamentous cyanobacteria. A third component to the phytoplankton assemblage is the diatom *Aulacoseira granulata* that in some years forms a deep-water bloom in January–February (Zohary, 2004). Macro-zooplankton biomass in Lake Kinneret is dominated for most of the year by herbivorous cladocerans (Gophen, 1984). The predatory zooplankton assemblage includes adult copepods, and large rotifers. The micro-zooplankton community includes copepod nauplii, small herbivorous and bactivorous rotifers, ciliates and heterotrophic flagellates (Hadas and Berman, 1998). A study of

stable carbon isotopes showed seasonal dietary variations of macro-zooplankton, with nanoplankton as the predominant food source (Zohary et al., 1994). The major food sources for the micro-zooplankton are bacteria and picophytoplankton for the smaller heterotrophic flagellates, and bacteria, heterotrophic flagellates and nanophytoplankton for the ciliates (Hadas and Berman, 1998; Madoni et al., 1990).

3. Methods

3.1. Model description

The model used in this study is a modified version of the Computational Aquatic Ecosystem Dynamics Model (CAEDYM) coupled to the Dynamic Reservoir Model (DYRESM). In DYRESM, the lake is represented as a series of homogeneous horizontal Lagrangian layers of variable thickness; as inflows and outflows enter or leave the lake, the affected layers expand or contract, respectively, and those above move up or down to accommodate any volume change. Mass, including that of the ecological state variables, is adjusted conservatively each time layers merge or are affected by inflows and outflows. The main processes modeled in DYRESM are surface heat, mass and momentum transfers, mixed layer dynamics, hypolimnetic mixing, benthic boundary layer mixing, inflows and outflows. Local meteorological data are used to determine penetrative heating due to short-wave radiation and surface heat fluxes due to evaporation, sensible heat, long-wave radiation and wind stress. The surface wind field introduces both momentum and turbulent kinetic energy to the surface layer contributing to vertical mixing. In addition to surface layer mixing, DYRESM includes algorithms that account for internal mixing (encompassing the effects of shear mixing energized by internal waves) and benthic boundary layer (BBL) mixing (determined by the turbulent kinetic energy budget and parameterized by Lake Number and the Burger number). In this way, mass transfer is enabled from hypolimnetic layers to the thermocline region via the BBL. A schematic flow chart of the operations performed in DYRESM is presented in Fig. 2. A detailed description of the processes included in DYRESM is given by Yeates and Imberger (2004).

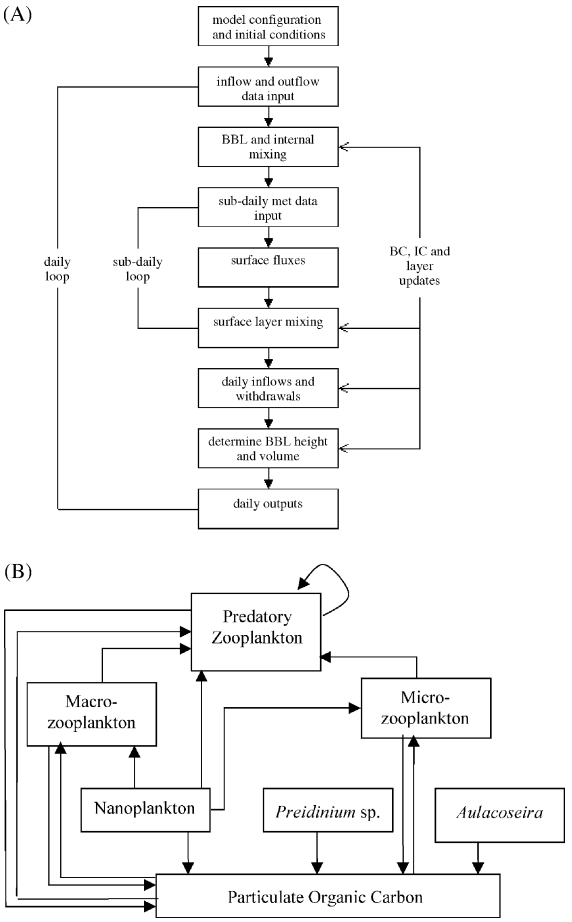

Fig. 2. Schematic representation of: (A) the physical processes included in the physical model DYRESM (BBL: benthic boundary layer; IC: internal cells; BC: benthic boundary layer cells) and (B) the carbon fluxes represented in the ecological model, CAEDYM.

The ecological model CAEDYM was set up in the form of a nutrients–phytoplankton–zooplankton ('N–P–Z') model, but with resolution to the level of individual species or groups of species (Griffin et al., 2000). In the present study, the model was used to simulate phosphorus and nitrogen in both particulate organic and dissolved inorganic forms (POP and PO_4, PON, NO_3 and NH_4), dissolved oxygen (DO), particulate organic carbon (POC), dissolved organic carbon (DOC), three phytoplankton groups and three zooplankton groups. The phytoplankton community was simulated using three groups in the model: "dinoflagellates", representing *P. gatunense*, "diatoms", representing *A. granulata*, and

Table 1
Equations used to describe the processes included in the ecological model CAEDYM

$\Delta P_j/\Delta t = [P_{max,j} f_1(T) \min(f(I), f(P), f(N)) - (R_j) f_2(T) - \text{Pred}_j]P_j \pm S_j$ = production − (respiration + excretion + mortality) − predation ± settling

$\Delta Z_i/\Delta t = [G_i A_i f(Z)_i f_1(T)(1 - f_{ex} - f_{eg}) - (R_i + M_i) f_2(T) - \text{Pred}_i]Z_i$ = (assimilation − excretion − egestion) − (respiration + mortality) − predation

$\Delta POC/\Delta t = \sum[G_i f(Z)_i f_1(T)_i((1 - A_i) + A_i f_{eg}) + M_i f_2(T)_i]Z_i + \sum[R_j(1 - f_{res})(1 - f_{DOM}) f_2(T)]P_j - \text{Pred}_{POM}POC - R_{POC} f(DO) f_1(T)POC \pm S_{POM}$ = (zooplankton messy feeding + zooplankton egestion + zooplankton mortality) + phytoplankton mortality − zooplankton predation − POC decomposition ± settling

$\Delta DOC/\Delta t = \sum[R_j(1 - f_{res}) f_{DOM} f_2(T)]P_j + R_{POC} f(DO) f_2(T)POC - R_{DOC} f(DO) f_2(T)DOC$ = phytoplankton excretion + POC decomposition − DOC mineralisation

$\Delta POP/\Delta t = \sum[G_i f(Z)_i f_1(T)_i((1 - A_i) + A_i f_{eg}) + M_i f_2(T)_i]IP_{Zi}Z_i + \sum[R_j(1 - f_{res})(1 - f_{DOM}) f_2(T)]IP_j - \text{Pred}_{POM}POP - R_{POP} f(DO) f_1(T)POP \pm S_{POM}$ = (unassimilated zooplankton food + zooplankton egestion + zooplankton mortality) + phytoplankton mortality − zooplankton predation − POP mineralisation ± settling

$\Delta PO_4/\Delta t = R_{POP} f(DO) f_2(T)POP - \sum[UP_{max,j} f_1(T)_j f(IP)_j f(P)_j]P_j + S_{dPO_4} f(DO) f_2(T)LA/LV =$ POP mineralisation − phytoplankton uptake + PO_4 sediment flux

$\Delta PON/\Delta t = \sum[G_i f(Z)_i f_1(T)_i((1 - A_i) + A_i f_{eg}) + M_i f_2(T)_i]IN_{zi}Z_i + \sum[R_j(1 - f_{res})(1 - f_{DOM}) f_2(T)]IN_j - \text{Pred}_{POM}PON - R_{PON} f(DO) f_1(T)PON \pm S_{POM}$ = (unassimilated zooplankton food + zooplankton egestion + zooplankton mortality) + phytoplankton mortality − zooplankton predation − PON mineralisation ± settling

$\Delta NH_4/\Delta t = R_{PON} f(DO) f_1(T)PON - \sum[UN_{max,j} P_N f_1(T)_j f(IN)_j f(N)_j]P_j - R_{NO} f(DO) f_2(T)NH_4 + S_{dNH_4} f(DO) f_2(T)LA/LV =$ PON mineralisation − phytoplankton uptake − nitrification + NH_4 sediment flux

$\Delta NO_3/\Delta t = R_{NO} f(DO) f_2(T)NH_4 - R_{N_2} f(DO) f_2(T)NO_3 - \sum[UN_{max,j}(1 - P_N) f_1(T)_j f(IN)_j f(N)_j]P_j =$ nitrification − denitrification − phytoplankton uptake

$\Delta DO/\Delta t = k_{O_2}(DOatm - DO) + \sum[P_{max,j} f_1(T)_j \min(f(I), f(P), f(N)) - R_j f_2(T)_j]P_j Y_{O_2:C} \sum[R_i f_2(T)_i]Z_i Y_{O_2:C} - R_{DOC} f(DO) f_1(T)DOCY_{O_2:C} - R_{NO} f(DO) f_2(T)NH_4 - S_{dDO} f(DO) f_2(T)LA/LV =$ atmospheric flux + (phytoplankton oxygen production − phytoplankton respiratory consumption) − zooplankton respiratory consumption − utilisation of oxygen in mineralisation of DOM − utilisation of oxygen in nitrification − sediment oxygen demand

Temperature functions

$f_1(T) = \theta^{T-20} - \theta^{k(T-a)} + b$

where k, a and b are constants solved numerically to satisfy the following conditions:

$f_1(T) = 1$, at $T = T_{sta}$

$\partial f_1(T)/\partial T = 0$, at $T = T_{opt}$

$f_1(T) = 0$, at $T = T_{max}$

$f_2(T) = \theta^{T-20}$

Limitation equations

$f(Z)_i = (\sum P_j + \sum Z_k + POC)/(K_i + \sum P_j + \sum Z_k + POC)$

$f(I)_j = I/I_s \exp(1 - I/I_s)$

$f(IP)_j = [IP_{max}/(IP_{max} - IP_{min})][1 - IP_{min}/IP]$

$f(IN)_j = [IN_{max}/(IN_{max} - IN_{min})][1 - IN_{min}/IN]$

$f(DO) = DO/(K_{DO} + DO)$

$f(P) = PO_4/(K_P + PO_4)$

$f(N) = (NH_4 + NO_3)/(K_N + NH_4 + NO_3)$

$P_N = (NH_4NO_3)/[(NH_4 + K_N)(NO_3 + K_N)] + (NH_4K_N)/[(NH_4 + K_N)(NO_3 + K_N)]$

Settling

$S_j = (ws/\Delta z)P_j$

$S_{POM} = (g(\rho_{POM} - \rho_w)(D_{POM})^2/18\mu)/\Delta z)POM$

Predation

$\text{Pred}_i = \sum(G_k f(Z)_k f_1(T)_k Z_k PzZOO_{k,i})$

$\text{Pred}_j = \sum(G_i f(Z)_i f_1(T)_i Z_i PzPHY_{i,j})$

$\text{Pred}_{POM} = \sum(G_i f(Z)_i f_1(T)_i Z_i PzPOC)$

Abbreviations: Z, zooplankton; P, phytoplankton; POC, particulate organic carbon; DOC, dissolved organic carbon; POP, particulate organic phosphorus; PO_4, phosphate; PON, particulate organic nitrogen; NH_4, ammonium; NO_3, nitrate; POM, particulate organic matter (C, N or P); IP_{zi}, zooplankton internal phosphorus; IN_{zi}, zooplankton internal nitrogen; IP_j, phytoplankton internal phosphorus; IN_j, phytoplankton internal phosphorus; DO, dissolved oxygen; DOatm, concentration of oxygen in the atmosphere; LA, layer area; LV, layer volume; Δz, layer thickness; ρ_w, density of water; μ, viscosity of water; k_{O_2}, oxygen transfer coefficient. *Subscripts*: i, zooplankton group; j, phytoplankton group; k, zooplankton predator group.

"nanoplankton" to account collectively for all other phytoplankton. The total zooplankton biomass was separated in the model into predatory zooplankton comprised of adult stages of cyclopoid copepods and the large rotifer *Asplanchna*, macro-zooplankton comprised of cladocerans and juvenile (copepodid) stages of copepods, and micro-zooplankton comprised of copepod nauplii, small rotifers and ciliates. CAEDYM uses a series of ordinary differential equations to describe changes in concentrations of nutrients, detritus, dissolved oxygen, phytoplankton and zooplankton as a function of environmental forcing and ecological interactions for each Lagrangian layer represented by DYRESM. Details of the structure of this model are given in Robson and Hamilton (2004) and Romero et al. (2004). Physical transport of ecological variables is carried out by DYRESM. The variables of irradiance, temperature, salinity and density are also passed to CAEDYM at each 1-h time step and used in equations to determine rates of change of biomass and chemical constituents for each of the ecological state variable. A conceptual diagram of the major ecological components and interactions represented in the model is shown in Fig. 2 and the main equations used in CAEDYM are listed in Table 1.

The major nutrient fluxes represented in CAEDYM are uptake of dissolved inorganic nutrients by phytoplankton, release of dissolved nutrients from phytoplankton excretion, grazing, egestion and excretion of nutrients by zooplankton, nitrification and denitrification of inorganic nitrogen, sedimentation of nutrients in particulate form, bacterially catalyzed mineralisation of organic nutrients and release of dissolved nutrients from bottom sediments (Table 1).

Net change in carbon concentration for each phytoplankton state variable at each model time step is calculated as the difference between the increment due to gross primary production and losses due to sedimentation, grazing by zooplankton, respiration, excretion and mortality. These terms are calculated using equations parameterized to represent the different physiologies of each phytoplankton group (Table 2). Losses due to grazing by zooplankton are calculated by multiplying the food assimilation rate for each zooplankton group by a preference factor for each food source.

Net zooplankton growth is calculated as a balance between food assimilation and losses from respiration, excretion, egestion, predation and mortality. Food assimilation is calculated as the product of the maximum potential rate of grazing, assimilation efficiency and temperature and food concentration functions. A constant internal nutrient ratio is assumed for simplicity, and excretion of nutrients is used to maintain this ratio at each time step. Advective movement of zooplankton is carried out in DYRESM. The mechanism of diel vertical migration is not considered to be important in the food web dynamics of Lake Kinneret (Easton and Gophen, 2003) and so was not included in the model.

Bacteria were not modeled explicitly due to scarcity of data and lack of parameter information, but the nutrient pathways catalyzed by bacteria were included in the mineralisation of the particulate organic pools (POC, POP and PON). Thus, the POC, POP and PON pools available for zooplankton grazing include bacteria also. Fish were not modeled explicitly; however, grazing of fish on phytoplankton and predation of fish on zooplankton were accounted for by calibrating the phytoplankton and zooplankton mortality terms using estimates of fish biomass and grazing and predation rates. Silica limitation of diatoms has not been observed in Lake Kinneret (Zohary, unpublished data), so this nutrient and its physiological effects were not included in the model.

3.2. Collection of field verification data

The main lake sampling station (station A) is located at the deepest point in the lake (Fig. 1). Data were chosen from this station for 1997 and 1998 because these years contained the most complete record for

Table 2A
Parameters used in CAEDYM to simulate ecological variable in Lake Kinneret—general

Parameter	Description	Units	Assigned value	Values from field/literature
K_d	Background extinction coefficient	m^{-1}	0.25	0.46[a], 0.25[b]

[a] Serruya and Berman (1976).
[b] Best fit to field data.

Table 2B
Parameters used in CAEDYM to simulate ecological variable in Lake Kinneret—phytoplankton

Parameter	Description	Units	Assigned values: *Peridinium*, nanoplankton, *Aulacoseira*	Values from field/literature
P_{max}	Maximum potential growth rate	day^{-1}	0.4 2.8 2.4	0.24–4.56[a] 2.4–8.57[a] 0.715[b]
I_s	Light saturation for maximum production	$\mu E\,m^{-2}\,s^{-1}$	130 75 440	130[c] 75[d] 440–710[b]
Kep	Specific attenuation coefficient	$m^2\,g\,C^{-1}$	0.449 0.54 0.448	0.449[e] 0.448[f]
K_P	Half saturation constant for phosphorus uptake	$mg\,L^{-1}$	0.002 0.0015 0.0015	0.001–0.0048[g] 0.0011[g] 0.0028–0.0111[g]
K_N	Half saturation constant for nitrogen uptake	$mg\,L^{-1}$	0.11 0.035 0.01	0.38[c]
IN_{min}	Minimum internal N ratio	$mg\,N\,(mg\,C)^{-1}$	0.0448 0.05 0.0766	0.0448[h] 0.125[g]
IN_{max}	Maximum internal N ratio	$mg\,N\,(mg\,C)^{-1}$	0.094 0.222 0.1125	0.09[h] 0.146[g]
UN_{max}	Maximum rate of nitrogen uptake	$mg\,N\,(mg\,C)^{-1}\,day^{-1}$	0.0448 0.111 0.109	0.0043[c]
IP_{min}	Minimum internal P ratio	$mg\,P\,(mg\,C)^{-1}$	0.0045 0.0061 0.0119	0.0040[h] 0.0119[g]
IP_{max}	Maximum internal P ratio	$mg\,P\,(mg\,C)^{-1}$	0.0187 0.0296 0.0850	0.0187[h] 0.0850[g]
UP_{max}	Maximum rate of phosphorus uptake	$mg\,P\,(mg\,C)^{-1}\,day^{-1}$	0.0033 0.0148 0.0125	0.0006-0.0060[g] 0.0074[g] 0.0031–0.0187[g]
θ_j	Temperature multiplier for growth		1.062 1.12 1.12	1.08[c] 1.06[b]
T_{sta}	Standard temperature	°C	20 20 20	
T_{opt}	Optimum temperature	°C	24 25 20	22[g] 20–30[g] 16–17[g]
T_{max}	Maximum temperature	°C	30 35 27.5	28[g] >35[g] 26–27[g]

Table 2B (*Continued*)

Parameter	Description	Units	Assigned values: *Peridinium*, nanoplankton, *Aulacoseira*	Values from field/literature
R_j	Metabolic loss rate coefficient	day^{-1}	0.02 0.03 0.01	0.03[c] 0.039–0.051[g]
θ_R	Temperature multiplier for metabolic loss		1.06 1.07 1.12	
f_{res}	Fraction of respiration relative to total metabolic loss		0.4 0.4 0.4	
f_{DOM}	Fraction of metabolic loss rate that goes to DOM		0.1 0.1 0.1	
ws	Settling velocity	ms^{-1}	0.0 1.74e−6 1.6e−5	 7e−6–1.15e−5[g]

[a] Pollingher and Berman (1982).
[b] Cole and Jones (2000).
[c] Pollingher (1986).
[d] Estimated from Reynolds (1984).
[e] Serruya and Berman (1976) (converted from Chl *a* units).
[f] Kirk (1994) (cited in Jewson, 1977—*Aulacoseira* in Lough Neagh, converted from Chl *a* units).
[g] Zohary (unpublished data).
[h] Wynne et al. (1982).

both model inputs (forcing data) and in-lake data. In addition, there were marked differences in phytoplankton assemblages between these 2 years that enabled us to rigorously evaluate both the validity of the model parameterization and patterns in model flux outputs.

Water samples were collected from station A with a 5-L bottle sampler from discrete depths (0, 1, 2, 3, 5, 7, 10, 15, 20, 30 and 40 m) between 08:00 and 10:00 h every 2 weeks for phytoplankton enumeration, and weekly for analysis of nutrient (TN, TP, PO_4-P, NO_3-N and NH_4-N) concentrations. The methods used for phytoplankton microscope counts, biovolume calculation and determination of fresh weight are described in Zohary (2004). As model simulations are based on phytoplankton carbon concentrations, wet weight (WW) was converted to carbon by assuming ratios of 0.155, 0.041 and 0.110 g C (g WW)$^{-1}$ for *Peridinium* sp., *Aulacoseira* sp. and nanoplankton, respectively, determined using a CHN analyzer (Zohary, unpublished data).

For routine determinations of copepod, cladoceran and rotifer biomass, composite water samples from discrete water column depths were taken every 2 weeks. Samples were collected every 5 m from the surface to the depth of the surface mixed layer that ranged from 16 m during stratification down to the bottom at 40 m during winter. All samples were mixed, fixed with formalin, and a sub-sample of 800 ml was taken for zooplankton counts. The counts were converted to biomass using values of mean wet weight per individual assuming a constant size within each taxonomic or life history group. Carbon content was estimated as 6% of wet weight for copepods (including all stages) and 8% of wet weight for cladocerans and rotifers (Hart et al., 2000). Ciliate biovolume was estimated assuming an oblate spheroidal shape and using a value of 0.14 pg C μm^{-3} to convert to equivalent carbon mass (Putt and Stockner, 1989). No ciliate data were available for the period 1997–1998, so multi-annual monthly means of data from 2001 to 2003 were used for both simulated years. Zooplankton were categorized as predatory zooplankton (predatory copepods and rotifers), macro-zooplankton (cladocerans and juvenile copepods) or micro-zooplankton (small herbivorous

Table 2C
Parameters used in CAEDYM to simulate ecological variable in Lake Kinneret—zooplankton

Parameter	Description	Units	Assigned values: predatory, macro, micro	Values from field/literature
G_i	Grazing rate	$g\,C\,m^{-3}\,(g\,C\,m^{-3})^{-1}\,day^{-1}$	1.1 1.67 2.5	1.0[a] 1.67[b] 2–10
A_i	Grazing efficiency	–	0.9 1.0 1.0	
R_i	Respiration rate coefficient	day^{-1}	0.08 0.08 0.25	0.32[a] 0.12[b] 0.32[a]
M_i	Mortality rate coefficient	day^{-1}	0.01 0.01 0.1	
f_{eg}	Fecal pellet fraction of grazing	day^{-1}	0.10 0.05 0.1	
f_{ex}	Excretion fraction of grazing	day^{-1}	0.3 0.11 0.2	0.13[a] 0.11[b]
DOmz	Minimum DO tolerance	$g\,O\,m^{-3}$	1.5 1.0 0.5	
θ_I	Temperature multiplier for growth		1.2 1.1 1.08	1.1[a] 1.15[b]
T_{sta}	Standard temperature	°C	20 20 20	20[a] 20[b]
T_{min}	Minimum temperature	°C	28 28 20	29[a] 28[b]
T_{max}	Maximum temperature	°C	38 34 27	34[a] 34[b]
θ_{R_i}	Respiration temperature dependence		1.05 1.15 1.15	1.1[a] 1.15[b]
K_i	Half saturation constant for grazing	$g\,C\,m^{-3}$	0.5 0.7 0.5	0.14[c] 0.54[d] 1.64[e]
IN_{zi}	Internal ratio of nitrogen to carbon	$g\,N\,g^{-1}\,C^{-1}$	0.2 0.2 0.2	0.184[f] 0.165[g]
IP_{zi}	Internal ratio of phosphorus to carbon	$g\,P\,g^{-1}\,C^{-1}$	0.01 0.01	0.005[f] 0.012[g]

Table 2C (*Continued*)

Parameter	Description	Units	Assigned values: predatory, macro, micro	Values from field/literature
			0.01	
PzPHY	Preference of zooplankton for nanoplankton		0.1	0.05[h]
			1.0	0.38[h]
			0.0	0.1[h]
PzZOO	Preference of zooplankton for predatory zooplankton		0.1	0.1[h]
			0.0	0.0[h]
			0.0	0.05[h]
PzZOO	Preference of zooplankton for macro-zooplankton		0.5	0.75[h]
			0.0	0.0[h]
			0.0	0.0[h]
PzZOO	Preference of zooplankton for micro-zooplankton		0.3	0.05[h]
			0.0	0.0[h]
			0.0	0.0[h]
PzPOC	Preference of zooplankton for POC		0.0	0.05[h]
			0.0	0.2[h]
			1.0	0.75[h]

[a] Gophen (1976a).
[b] Gophen (1976b).
[c] Landry and Hassett (1985), *Calanus pacificus*.
[d] Haney and Trout (1985), *Ceriodaphnia quadrangular*.
[e] Stemberger and Gilbert (1985), *Asplanchna priodonta*.
[f] Andersen and Hessen (1991), *Acanthodiaptomus denticornis* mean.
[g] Andersen and Hessen (1991), *Daphnia longispina* mean.
[h] Gophen and Azoulay (2002).

and bactivorous rotifers, ciliates and flagellates). Micro-zooplankton data were used for comparative purposes only and not for measures of model fit due to paucity of flagellate data and the fact that samples were collected outside of the simulated period.

Particulate organic carbon concentration in the water was approximated from measurements of total suspended solids (TSS) using the following equation:

$$\mathrm{POC} = \mathrm{TSS} \times 0.5 \times \mathrm{LI} \quad (1)$$

where LI is the proportion of C lost from filter combustion for 1 h at 550 °C, representing organic matter, and assuming that C is 0.5 of the weight of organic matter. LI values varied from 0.6 during diatom blooms to 0.925 during *Peridinium* blooms, and 0.8 for the rest of the year (A. Parparov, personal communication, 2004).

3.3. Model inputs

Model input files include data for initialization, meteorology, inflows and outflows. The initialization file was prepared from field data collected on 5 January 1997. Inflow data included the daily volume, temperature, salinity and nutrient concentrations of each inflow. Phytoplankton and zooplankton concentrations were negligible in the inflows and were set to zero. The outflow file included the total daily outflow volume from released outflow and local pumping. Meteorological input data included hourly short- and long-wave radiation, air temperature, vapor pressure, wind speed and precipitation collected from a meteorological station located at Tabgha (Fig. 1) approximately 1 km from the northwest shore of the lake (see Gal et al., 2003).

The physical parameters used to simulate the hydrodynamics of Lake Kinneret were either physical constants or were fixed according to the dimensions of the lake (Yeates and Imberger, 2004).

Parameters used for CAEDYM are listed in Table 2. Most parameters were derived from recent experimental analyses on the three phytoplankton groups (Zohary, unpublished data) and three zooplankton groups (Hambright, unpublished data) from the lake, as well as

Table 2D
Parameters used in CAEDYM to simulate ecological variable in Lake Kinneret—dissolved oxygen and nutrients

Parameter	Description	Units	Assigned values	Values from field/literature
$Y_{O_2:C}$	Stoichiometric ratio of oxygen to carbon	–	2.6667	
S_{dDO}	DO sediment exchange rate	$g\,O\,m^{-2}\,day^{-1}$	1.5	
K_{DO_sed}	Half saturation constant for DO sediment flux	$g\,O\,m^{-3}$	0.5	
K_{DO_POM}	Half saturation constant for dependence of POM/DOM decomposition on DO	$g\,O\,m^{-3}$	2.5	
fanB	Aerobic/anaerobic factor	–	0.3	
θ_{POM}	Temperature multiplier	–	1.18	1.02–1.14[a]
R_{POC}	Mineralisation rate for POC to DOC	day^{-1}	0.001	
R_{POP}	Mineralisation rate for POP to PO_4	day^{-1}	0.01	0.01–0.1[a]
R_{PON}	Mineralisation rate for PON to NH_4	day^{-1}	0.02	0.01–0.03[a]
D_{POM}	Diameter of POM particles	m	0.0000150	
ρ_{POM}	Density of POM particles	$kg\,m^{-3}$	1080	
KePOC	Specific light attenuation coefficient for POC	$m^2\,g^{-1}$	0.001	
R_{DOC}	Mineralisation rate for DOC	day^{-1}	1	Set to 1 to eliminate DOC pool for simplicity
KeDOC	Specific light attenuation coefficient of DOC	$m^2\,g^{-1}$	0.001	
R_{N_2}	Denitrification rate coefficient	day^{-1}	0.08	0.1[a]
θ_{N_2}	Temperature multiplier for denitrification	–	1.08	1.045[a]
K_{N_2}	Half saturation constant for denitrification dependence on oxygen	$g\,N\,m^{-3}$	0.5	
R_{NO}	Nitrification rate coefficient	day^{-1}	0.015	0.1–0.2[a]
θ_{NO}	Temperature multiplier for nitrification	–	1.08	1.08[a]
K_{NO}	Half saturation constant for nitrification dependence on oxygen	$g\,O\,m^{-3}$	0.5	
θ_{sed}	Temperature multiplier for sediment nutrient fluxes	–	1.05	
S_{dPO_4}	Release rate of PO_4 from sediments	$g\,m^{-2}\,day^{-1}$	0.0008	0.0008[b]
$K_{DO\_S_{dPO_4}}$	Controls sediment release of PO_4 via oxygen—half saturation constant for sediment PO_4 release dependence on DO	$g\,m^{-3}$	3.0	
S_{dNH_4}	Release rate of NH_4 from sediments	$g\,m^{-2}\,day^{-1}$	0.05	0.025[b]
$K_{DO\_S_{dNH_4}}$	Controls sediment release of NH_4 via oxygen—half saturation constant for sediment NH_4 release dependence on DO	$g\,m^{-3}$	1.0	

[a] Jorgensen and Bendoricchio (2001).
[b] Serruya et al. (1974).

published literature and reports on the biota of Lake Kinneret. Where parameters were not available, a series of model runs were performed to calibrate the simulation results against field data, maintaining parameter values within the bounds of literature values for the same or similar species in other lakes.

The period from January to April 1997 was used for initial parameter calibration. Half-saturation constants for zooplankton grazing strongly influenced the timing and magnitude of peaks in phytoplankton and zooplankton biomass. For each zooplankton group these parameters were adjusted within ranges of published literature, to reproduce the observed mid-winter and spring peaks of the predatory and macro-zooplankton groups, and winter growth and mid-spring peaks of micro-zooplankton. The remainder of 1997 was used to make minor adjustments to parameters (e.g. grazing and losses) in order to reproduce observed seasonal variations while the 1998 period was used for model validation.

Comparisons of field and model data were made for monthly averaged photic zone concentrations (surface 10 m). Definition of what would be considered a "good" or "acceptable" fit is difficult to establish quantitatively and we choose representation of closeness of model fit using the average absolute error normalized to the mean

(NMAE; Alewell and Manderscheid, 1998):

$$\mathrm{NMAE} = \frac{\sum_{t=1}^{n}(|s_t - o_t|)}{n\bar{o}}, \quad (2)$$

where s_t is the simulated value at time t, o_t the observed value at time t, $\bar{o}$ the mean of the observed values over the simulation period and n is the number of observed values. NMAE is a measure of the absolute deviation of simulated values from observations, normalized to the mean; a value of zero indicates perfect agreement and greater than zero an average fraction of the discrepancy normalized to the mean. Since an acceptable fit depends on the scatter of the observed data, we calculated, from the field data for each state variable, a standard deviation from monthly averages. As a comparison to overall model fit, these monthly standard deviations were then averaged over the simulation period and normalized to the mean (see Table 3). Model fit was considered acceptable when the simulated NMAE's fell within or close to one standard deviation of the observed monthly average field data.

Although the NMAE method gives useful quantitative information about model performance, it may misrepresent the fit in cases where the mean is very small compared with a short-term peak or bloom (Alewell and Manderscheid, 1998). Values of NMAE were therefore combined with qualitative graphical comparisons in evaluating the success of the calibration procedure.

A sensitivity analysis was performed on each of the CAEDYM parameters listed in Table 2, adjusting each parameter by ±10% or by ±0.01 in the case of the temperature multipliers. Sensitivity coefficients (s_{ij}) to assess the relative sensitivity of variable i to parameter j were calculated according to Chen et al. (2002):

$$s_{ij} = \frac{\Delta c_i / \bar{c_i}}{\Delta \beta_j / \bar{\beta_j}} \quad (3)$$

where Δc_j is the change in variable i from the reference value c_i and $\Delta \beta_j$ is the change in parameter j from the reference value β_j. The calculations were made for each of the major state variables taking the daily mean photic depth concentrations averaged over the full simulation period.

Table 3
Results of normalized mean absolute error (NMAE) calculations applied to compare simulated to field data for years 1997–1998

Variable	NMAE	S.D./mean
Dissolved oxygen	0.07 (0.09)	0.07 (0.06)
NH_4	0.66 (0.68)	0.40 (0.44)
NO_3	0.43 (0.32)	0.27 (0.20)
PO_4	0.81 (0.81)	0.66 (0.91)
Nanoplankton	0.50 (0.41)	0.37 (0.41)
Peridinium	0.40 (0.51)	0.41 (0.44)
Aulacoseira	0.79 (0.49)	0.68 (0.89)
Predatory zooplankton	0.59 (0.51)	0.50 (0.46)
Macro-zooplankton	0.46 (0.35)	0.31 (0.20)
Micro-zooplankton	0.85 (0.88)	–
Average	0.52 (0.46)	0.41 (0.45)

The values in parentheses represent the same calculations made over the 1997 calibration period.

4. Results

Dissolved oxygen in the upper 10 m measured in the field is elevated through the first 6 months of both years, with a peak in May–April corresponding to increased phytoplankton biomass as a result of *Peridinium* blooms (Fig. 3). The simulated data show a similar pattern although peak values are slightly lower than in the field. The inorganic nitrogen field data for the upper 10 m of water column show a strong seasonal pattern with increased concentrations in the winter months following the breakdown in stratification, and low concentrations during the summer stratified period (Fig. 3). The NO_3 peak and subsequent decline in the field data followed a similar sequence, but with a 1–2 month phase lag compared with NH_4 (Fig. 3). The lag may be explained by nitrification of NH_4 to NO_3 at turnover, following the progressive build up of NH_4 in the hypolimnion during the stratified period. NO_3 subsequently declined in the surface layer as inorganic nutrients were depleted through biological uptake (Fig. 3). The simulated results showed a similar pattern although the summer decline of NO_3 in 1997 was slower than observed in the field and the NH_4 peak in the 1997–1998 winter was slightly delayed (Fig. 3). The PO_4 field data varied irregularly in 1997, declined to low concentrations in the first 3 months of 1998 and then showed elevated concentrations throughout the remainder of 1998 (Fig. 3). A period of increased concentration following the breakdown of stratification in December 1997 was captured with the model simulations, as well as the elevated concentrations in the second half of 1998, but the model otherwise tended

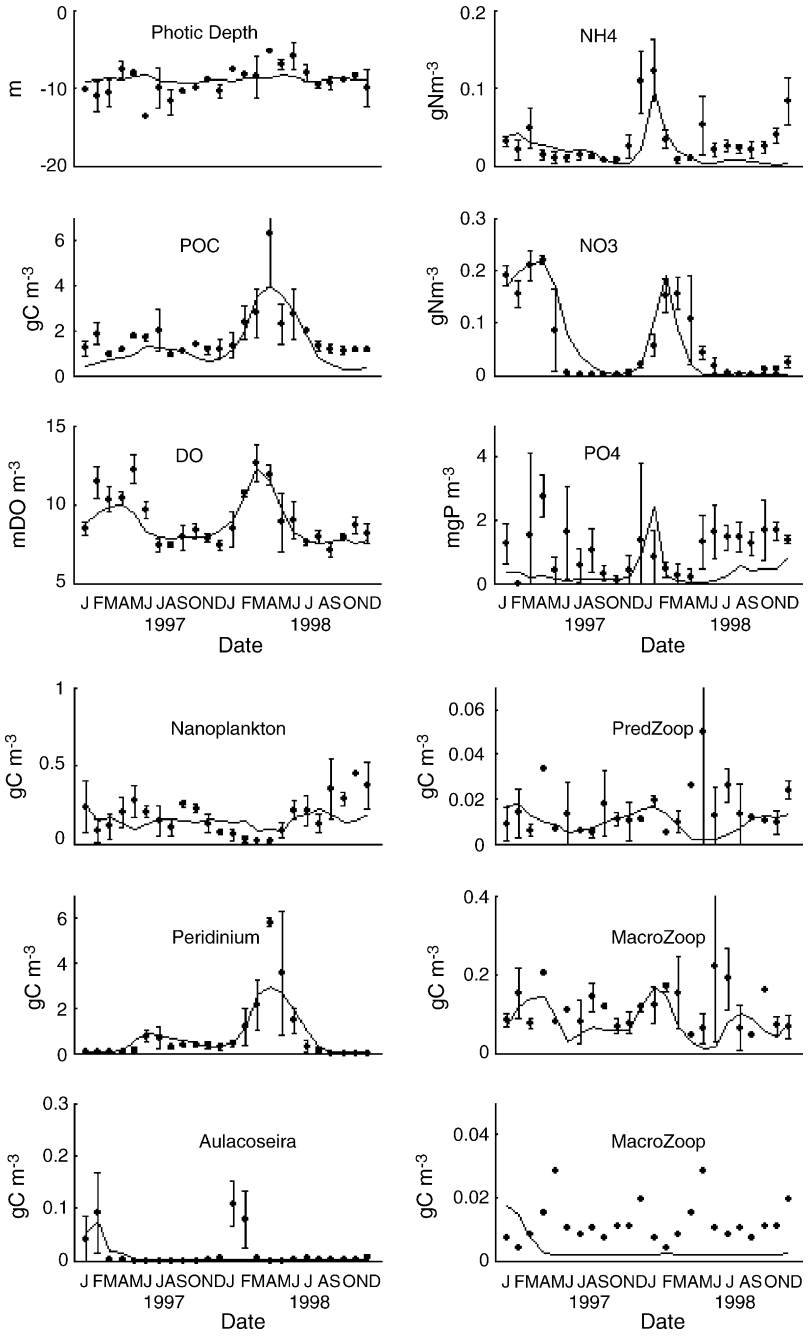

Fig. 3. Comparison of monthly averages of model simulation results (continuous line) and field data (circles) for Lake Kinneret in 1997 and 1998 for nutrients (NH_4, NO_3 and PO_4), phytoplankton (nanoplankton, *Peridinium* and *Aulacoseira*), photic depth, POC, DO and zooplankton (predatory, macro and micro). The error bars on the field data indicate the standard deviation from the mean for each month.

to underestimate PO_4 concentrations (Fig. 3). Despite this discrepancy, the simulation results of the major (in term of biomass) phytoplankton species (nanoplankton and *Peridinium*) generally closely followed the trends in the field data.

The nanoplankton field and simulated data exhibit a similar pattern to the PO_4 data, with concentrations that were variable in 1997, decreased in early 1998 and were then elevated for the remainder of 1998 (Fig. 3). The *Peridinium* field data show two peaks: one in 1997 and one in 1998 (Fig. 3). The 1997 peak occurred later (June–July) and was seven times lower than the peak in June 1998 which was the end-point of a continuous increase from February 1998 (Fig. 3). The other major difference between the years was that, although some *Peridinium* biomass persisted through the second half of 1997, there was little biomass in the second half of 1998. These patterns were captured well in the simulated data (Fig. 3). Large increases in *Aulacoseira* biomass occurred in January and February of both 1997 and 1998. The simulated results did not reproduce the bloom in 1998 but the C-biomass contributed by *Aulacoseira* was small (3% of total) and of lesser importance to the role of zooplankton, that generally do not graze this large filamentous diatom (Fig. 3). The timing and magnitude of the peaks may be related to resuspension of resting cells caused by high turbulence (Zohary, 2004) while the decline may be related to the re-establishment of the stratification and enhanced sedimentation losses of cells. Resuspension of resting cells was not simulated in the model, which may explain the absence of an *Aulacoseira* bloom in the 1998 simulated results, while the initial conditions prescribed for January 1997 ($0.025\ g\ C\ m^{-3}$) stimulated a bloom prior to stratification.

Biomass of predatory zooplankton in Lake Kinneret showed reasonable scatter punctuated by a short-duration peak in April 1997 and a larger peak from April to May 1998 (Fig. 3). The magnitude of these variations was captured by the model simulations but the peak in June 1998 was not reproduced (Fig. 3). The field data for the macro-zooplankton biomass were almost 10 times higher than for the predatory zooplankton. It is difficult to discern obvious seasonal patterns in the field data although concentrations were elevated mid-summer and mid-winter, which were captured in the simulations (Fig. 3). The micro-zooplankton field data were compiled by averaging monthly biomass measurement for years 2001–2003, so there is no inter-annual variation (Fig. 3) but there is a peak in concentration for the months of April and May. These peaks were not captured in the model data, and the simulated concentrations for the remainder of both years were lower than the field data (Fig. 3). Although the contribution of micro-zooplankton to total zooplankton biomass is small, this group has high growth and excretion rates, so their contribution to lake nutrient fluxes is most probably underestimated.

It is possible that discrepancies between model and field data may be the result of misrepresentation of field data associated with bias from sampling concentrated patches of zooplankton (see Yacobi et al., 1993). The errors associated with spatial and temporal variations are reflected in the error bars representing the standard deviation calculated from samples taken at different times in the lake (Fig. 3); high spatial variability is evident where the standard deviation exceeds the mean value (e.g. predatory zooplankton in June 1998). In the cases where spatial variation is not so evident (e.g. *Peridinium*, January–December 1997), simulated and observed data are generally in good agreement. In these cases, the use of a spatially averaged model is more appropriate.

In summary, the model appeared to simulate all the variables within the bounds of the scatter in the field data. The only major exception to this was micro-zooplankton where the model simulations were consistently too low after the initial calibration period. As explained above, the micro-zooplankton were characterized by a high turnover of biomass so that achieving a balance between growth rate and respiration was difficult. Current data collection of micro-zooplankton has improved and future work will focus on the role of the micro-zooplankton in the nutrient cycles of the lake.

In both 1997 and 1998, the field data indicate that anoxia occurs in the hypolimnion from June to November or December, below a depth of approximately 20 m (Fig. 4C). This pattern was well reproduced by the model although the oxygen depletion extended vertically faster in the field than in the model. Based on the comparison of field and simulated temperatures (Fig. 4A and B, respectively), the extent of mixing through the water column is well reproduced, but the discrepancy in the oxygen contour plots (Fig. 4C and D) suggests that the water column oxygen depletion, determined through interactions of mixing, consump-

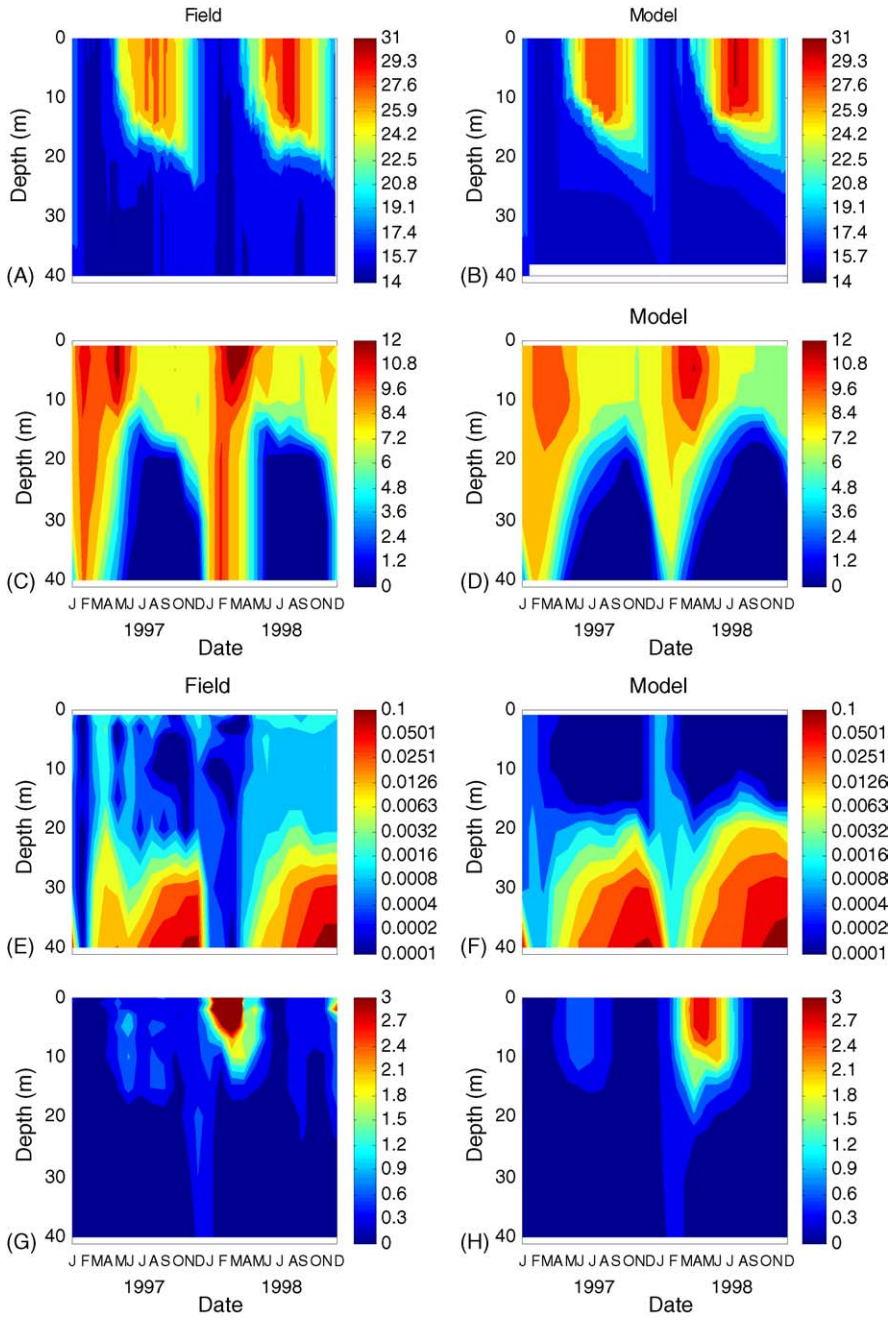

Fig. 4. Comparative contour plots for measured and simulated temperatures (A and B), dissolved oxygen (C and D), PO_4 (E and F) and total phytoplankton carbon (G and H) for 1997–1998.

tion and photosynthetic production of oxygen, may require further study and refinement. The pattern of stratification and anoxia is also reflected in increased release rates of PO_4-P during anoxia (see Fig. 7A) resulting in PO_4 build up in the hypolimnion prior to breakdown of stratification at which point it is rapidly vertically redistributed (Fig. 4E and F). For the case of the observed total phytoplankton carbon (Fig. 4G), elevated concentrations occur from May to August 1997 and to an even greater extent from February to June 1998. For the simulated results, the timing of these patterns is well matched although the magnitude is ∼30% lower for the summer bloom of 1998 (Fig. 4H).

4.1. Quantitative measures of model fit

The calculated values of normalized mean absolute error are presented in Table 3 for each of the major state variables over the full simulation period from 1997 to1998. They all fall within or close to the normalized mean standard deviation of the field data with the exception of NH_4 and NO_3. Although the NMAE values for the simulated results were generally higher for the full simulation period (1997–1998) than for the calibration period (1997), the increases were comparatively low, indicating that in general, the model provides a robust prediction beyond the 1997 calibration period.

4.2. Sensitivity analysis

To evaluate which parameters have the greatest effect on model results, sensitivity coefficients (s_{ij}, Eq. (3)) (a relative measure of sensitivity of outcome related to parameter change) were calculated for each of the major state variables and presented in Table 4. Chen et al. (2002) defined a parameter to be sensitive if the s_{ij} was >0.5. Using this definition, the percentage of sensitive parameters (highlighted in bold) for each variable was calculated and included in the last row of Table 4. Of nine variables, four (NO_3, nanoplankton, *Aulacoseira* and macro-zooplankton) had less than 10% of parameters sensitive, three (NH_4, *Peridinium* and micro-zooplankton) had approximately 30% and two (PO_4 and predatory zooplankton) had the majority of parameters sensitive to their outcome. A s_{ij} value greater than 1 means that the percentage change in simulated variable is greater than the percentage change in the parameter; in other words, the parameter change is leveraged by the model.

The greatest number of sensitive parameters relate to the prediction of PO_4, *Peridinium* and predatory zooplankton concentrations. Macro-zooplankton and micro-zooplankton had a smaller number of parameters sensitive to their prediction. The parameters that had the greatest s_{ij} averaged from all variables were the grazing rate, assimilation efficiency and standard temperature of the predatory zooplankton. These were followed by the half saturation constant for grazing, and the maximum (limiting) temperature of the macro-zooplanton. Another very sensitive parameter was the POM density which directly affects the settling loss of POC, POP and PON from the water column.

4.3. Trophic dynamics

Simulations of the total carbon mass generally compared favorably with field data although simulated total biomass is consistently lower than the field (Fig. 5A and B). This is mainly due to low simulated values of POC. Since the field POC data were estimated by first converting TSS to POC and then subtracting the phytoplankton data (Eq. (1)), field data may include a refractory component not included in the model. In April 1998, there was an exceptionally large *Peridinium* bloom, the peak concentration of which was not well captured by the model (see also Fig. 3). In both 1997 and 1998, the total carbon mass measured in the field and simulated by the model increased during mixis, peaked in early summer and then declined towards the end of the stratified period (Fig. 5A and B). In both the field and the model simulation results, the zooplankton biomass represented an average of approximately 10% of the total carbon biomass (Fig. 5C and D). In the field data the detrital POC component of total carbon, including bacterial biomass, ranges from ca. 75% in August 1998, when phytoplankton biomass was low, to nearly zero in May 1998 during the *Peridinium* bloom (Fig. 5C). In this case, the POC data in the field may have been underestimated by removing an overestimate of phytoplankton carbon and are likely to be closer to those estimated from the simulation results during this period.

Five major whole-lake carbon fluxes were extracted from the model and normalized with respect to the lake's surface area: (1) gross primary productivity; (2)

Table 4
Results of sensitivity analysis on parameters used in CAEDYM to simulate Lake Kinneret

Parameter	NH_4	NO_3	PO_4	Peri	Nano	Aula	Pred	Macro	Micro	Ave
K_d	−0.36	−0.14	0.44	−0.41	−0.07	−0.38	−1.18	0.11	−0.51	0.40
P_{max}	−0.63	−0.35	−0.76	1.41	−0.10	−0.10	−1.66	−0.47	−0.18	0.63
	−0.48	−0.25	−0.12	−0.75	0.00	−0.47	−0.20	0.30	−0.14	0.30
	−0.27	−0.06	1.08	0.13	−0.02	1.06	−0.89	0.11	−0.35	0.44
I_s	−0.40	−0.14	−0.38	−0.22	−0.08	−0.08	−0.88	−0.06	−0.49	0.30
	−0.32	−0.12	0.22	0.20	−0.07	0.00	−1.12	−0.03	−0.24	0.26
	0.03	0.04	−0.20	−0.72	0.03	−0.43	0.06	0.07	−0.55	0.24
Kep	−0.02	0.06	−0.63	−0.53	0.04	0.08	0.07	0.03	−0.60	0.23
	0.17	0.13	1.41	−0.02	0.01	−0.31	−0.32	0.13	−0.83	0.37
	−0.58	−0.19	−1.30	−0.01	−0.06	−0.10	−0.82	−0.21	−0.05	0.37
K_P	−0.05	0.15	−0.99	−1.91	0.05	−0.02	0.58	0.16	−0.88	0.53
	−0.40	−0.26	0.29	1.13	−0.03	0.40	−1.23	−0.23	−0.26	0.47
	−0.35	−0.18	−0.23	−0.07	−0.09	−0.29	−0.96	−0.04	−0.51	0.30
K_N	−0.40	−0.24	−0.69	0.07	−0.06	−0.02	−1.06	0.08	−0.43	0.34
	−0.27	−0.28	−1.53	0.16	−0.06	−0.10	−0.86	−0.13	−0.24	0.40
	−0.41	−0.14	0.20	−0.09	−0.04	0.09	−0.89	−0.04	−0.78	0.30
IN_{min}	−0.37	−0.17	0.17	−0.48	−0.05	−0.09	−0.83	0.04	−0.53	0.30
	−0.70	−0.37	0.65	−0.04	−0.05	−0.07	−1.02	−0.14	−0.46	0.39
	−0.11	−0.12	0.20	−0.08	0.03	−0.35	−0.05	0.12	−0.24	0.14
IN_{max}	−0.32	−0.22	−0.31	−0.21	−0.02	−0.06	−0.48	−0.11	−0.60	0.26
	−0.68	−0.74	0.80	−0.61	−0.07	−0.08	−0.67	0.01	−0.20	0.43
	−0.54	−0.22	−0.61	−0.03	−0.09	0.04	−1.19	−0.19	−0.51	0.38
UN_{max}	−0.62	−0.26	−0.10	−0.11	−0.05	0.05	−0.59	0.01	0.16	0.22
	−0.67	−0.46	1.30	−0.40	−0.04	0.01	−0.81	−0.01	−0.28	0.44
	−0.44	−0.18	**−2.28**	−0.58	−0.08	−0.09	−0.77	−0.38	−0.56	0.59
IP_{min}	−0.16	0.10	1.18	**−2.61**	−0.03	0.02	−0.19	0.22	−0.63	0.57
	−0.58	0.03	−0.81	0.82	−0.16	0.62	**−2.28**	−0.67	−0.02	0.67
	−0.53	−0.21	−1.28	−0.09	−0.09	−0.98	−1.12	−0.12	−0.53	0.55
IP_{max}	−0.75	−0.30	−0.45	0.06	−0.09	−0.09	−1.27	−0.02	−0.47	0.39
	−0.67	−0.20	−0.85	−0.52	−0.07	−0.04	−0.88	−0.12	0.01	0.37
	−0.27	−0.04	−0.56	−0.18	−0.06	−0.03	−1.05	−0.06	0.05	0.26
UP_{max}	−0.83	−0.35	−0.52	1.30	−0.10	0.00	−1.88	−0.46	−0.43	0.65
	−0.18	0.09	−0.98	**−2.04**	0.04	−0.52	0.38	0.21	−0.59	0.56
	−0.25	−0.05	−1.09	−0.32	−0.06	0.50	−0.96	−0.06	−0.54	0.43
θ_j	−0.33	−0.15	0.86	−0.12	0.00	−0.15	−0.21	0.29	−0.67	0.31
	−0.55	−0.09	−0.35	−0.25	−0.06	0.23	−1.29	−0.36	−0.01	0.35
	0.00	0.00	0.00	0.00	0.00	0.00	0.00	0.00	0.00	0.00
T_{sta}	−0.23	−0.08	−0.78	0.24	−0.02	0.00	−0.31	−0.11	−0.03	0.20
	−0.08	−0.05	1.53	−1.31	0.06	0.01	0.58	0.49	−0.01	0.46
	0.00	0.00	0.00	0.00	0.00	0.00	0.00	0.00	0.00	0.00
T_{opt}	0.00	0.00	0.00	0.00	0.00	0.00	0.00	0.00	0.00	0.00
	−0.28	−0.08	−0.13	−0.77	0.01	0.00	0.28	0.23	0.04	0.20
	0.00	0.00	0.00	0.00	0.00	0.00	0.00	0.00	0.00	0.00
T_{max}	−0.34	−0.09	−1.15	**2.06**	−0.05	−0.01	−1.48	−0.57	−0.01	0.64
	−0.15	0.00	0.58	−0.30	−0.01	0.00	−0.10	−0.16	−0.03	0.15
	0.00	0.00	0.00	0.00	0.00	0.00	0.00	0.00	0.00	0.00

Table 4 (*Continued*)

Parameter	NH_4	NO_3	PO_4	Peri	Nano	Aula	Pred	Macro	Micro	Ave
R_j	0.31	0.28	0.91	**−2.59**	0.04	0.00	0.58	0.37	0.06	0.57
	−0.26	−0.10	1.60	0.52	−0.07	0.15	−1.15	−0.26	0.23	0.48
	0.42	0.25	0.57	−0.43	0.04	−0.23	0.00	0.12	−0.23	0.25
θ	−0.46	−0.14	−1.36	−1.14	−0.07	0.09	−0.52	−0.12	−0.44	0.48
	−0.31	−0.17	0.36	0.06	−0.06	−0.08	−1.04	0.04	−0.36	0.28
	−0.50	−0.09	−1.80	−0.61	−0.14	0.13	−0.82	−0.40	0.26	0.53
f_{res}	−0.17	−0.14	0.41	−0.01	0.02	−0.06	−0.18	0.05	−0.39	0.16
	−0.43	−0.14	−0.42	−0.56	−0.04	−0.06	−0.60	−0.04	−0.19	0.28
	−0.38	−0.09	−1.03	−0.13	−0.09	−0.12	−1.21	−0.06	−0.51	0.40
f_{DOM}	−0.22	−0.09	−0.93	−0.09	−0.03	−0.05	−0.73	0.01	0.09	0.25
	−0.30	−0.11	0.15	0.14	−0.05	0.07	−0.90	0.05	−0.48	0.25
	−0.53	−0.16	0.18	−0.23	−0.05	0.04	−0.84	−0.16	−0.26	0.27
ws	0.00	0.00	0.00	0.00	0.00	0.00	0.00	0.00	0.00	0.00
	−0.58	−0.21	−0.81	−0.23	−0.10	−0.07	−1.45	−0.22	0.06	0.41
	−0.29	−0.08	**2.04**	−0.17	0.01	−1.53	0.12	−0.09	−0.29	0.51
G_i	−1.98	−0.24	**−3.91**	**−8.21**	1.81	−0.23	**30.21**	**−4.61**	−0.21	**5.71**
	−0.05	−0.04	−0.09	**2.63**	−0.77	0.95	**−4.14**	−0.10	−0.98	1.08
	−0.32	−0.15	0.32	0.12	−0.04	−0.07	−0.74	−0.06	**2.36**	0.46
A_{zi}	−1.77	−0.24	**−3.97**	**−7.96**	1.99	−0.12	**34.76**	**−4.66**	−0.72	**6.24**
	0.08	0.26	−0.31	**3.06**	−0.76	0.68	**−3.45**	0.88	**−2.17**	1.30
	−0.46	−0.16	−0.74	−0.14	−0.07	−0.08	−1.10	−0.06	**2.49**	0.59
R_i	−0.36	−0.31	−1.34	**2.01**	−0.26	0.02	**−4.81**	0.15	−0.84	1.12
	−0.58	−0.06	**−2.91**	**−3.73**	0.93	−0.05	**8.20**	−1.89	−0.11	**2.05**
	−0.55	−0.16	−1.07	−0.45	−0.06	0.10	−0.97	−0.14	−1.28	0.53
M_i	−0.69	−0.38	−0.31	0.66	−0.13	0.00	**−2.36**	0.15	−0.36	0.56
	−0.37	−0.06	−0.83	−0.58	−0.02	−0.13	−0.92	−0.22	0.03	0.35
	−0.23	−0.14	−0.79	−0.26	−0.01	0.04	−0.29	−0.07	−0.78	0.29
f_{eg}	−0.57	−0.22	−1.71	0.61	−0.16	−0.01	−1.99	−0.22	−0.46	0.66
	−0.54	−0.25	−0.68	−0.30	0.02	−0.05	−0.67	−0.19	−0.08	0.31
	−0.67	−0.25	0.40	−0.10	−0.07	−0.08	−0.86	−0.13	−0.18	0.31
f_{ex}	−0.35	−0.15	−0.89	1.11	−0.15	−0.06	**−3.13**	0.02	−0.72	0.73
	−0.16	0.09	−1.38	−0.58	0.07	0.02	0.26	−0.41	−0.45	0.38
	−0.61	−0.12	**−2.37**	−0.67	−0.10	−0.03	−0.87	−0.43	−0.58	0.64
DOmz	−0.27	−0.09	0.00	0.03	−0.03	−0.09	−0.35	−0.05	−0.54	0.16
	−0.19	−0.03	−0.98	−0.26	0.02	0.00	0.04	−0.25	0.06	0.20
	−0.12	0.07	−0.52	−0.10	−0.02	−0.09	−0.24	−0.14	−0.47	0.20
θ_j	−0.34	−0.18	−0.99	0.52	−0.14	0.07	**−2.41**	0.03	−0.50	0.57
	−0.19	−0.03	−0.77	−1.13	0.22	−0.18	1.20	−0.31	−0.34	0.48
	−0.45	−0.09	−0.50	−0.27	−0.08	−0.09	−1.12	−0.06	−0.76	0.38
T_{sta}	−1.28	−0.08	**−3.66**	**−5.96**	1.31	−0.01	**26.33**	**−3.76**	−0.06	**4.72**
	−0.36	−0.13	−1.47	0.89	−0.34	−0.01	**−2.23**	−0.34	0.06	0.65
	−0.36	−0.07	−1.24	−0.25	0.02	0.00	−0.13	−0.25	0.65	0.33
T_{min}	−0.34	0.02	0.16	−1.26	0.14	0.00	1.99	−0.38	−0.03	0.48
	−0.31	−0.15	−1.02	**2.66**	−0.97	−0.01	**−4.14**	−0.47	−0.07	1.09
	−0.26	−0.06	1.28	0.00	−0.03	0.00	−0.19	−0.17	0.11	0.23
T_{max}	−0.29	−0.16	0.14	0.21	−0.04	0.00	−0.87	0.01	0.17	0.21
	−0.95	−0.01	**−3.45**	**−4.81**	1.32	−0.01	**16.47**	**−2.53**	−0.09	**3.29**
	−0.19	−0.04	−0.17	−0.08	−0.02	0.00	−0.13	−0.06	−0.02	0.08

Table 4 (*Continued*)

Parameter	NH_4	NO_3	PO_4	Peri	Nano	Aula	Pred	Macro	Micro	Ave
θ_{R_i}	−0.41	−0.16	1.21	0.47	−0.12	0.00	**−2.20**	0.19	−0.45	0.58
	−0.52	0.02	−0.26	−1.58	0.33	−0.02	1.84	−0.37	−0.82	0.64
	−0.80	−0.30	−1.77	−0.37	−0.09	−0.04	−0.74	−0.42	0.85	0.60
K_i	−0.38	−0.32	−0.71	1.55	−0.25	−0.07	**−4.46**	0.18	−0.56	0.94
	−0.97	−0.06	**−3.69**	**−7.07**	**2.07**	−0.70	**24.28**	**−3.51**	−0.54	**4.76**
	−0.42	−0.21	0.67	−0.34	0.03	−0.07	−0.08	0.08	−1.42	0.37
IN_{zi}	0.25	0.11	0.67	−0.37	0.03	−0.06	−0.32	0.18	−0.51	0.28
	−0.74	−0.45	0.56	0.21	−0.03	0.00	−0.78	0.03	0.05	0.32
	−0.43	−0.13	0.10	−0.24	−0.07	−0.16	−1.09	−0.04	−0.54	0.31
IP_{zi}	−0.34	−0.17	1.08	0.29	−0.12	−0.08	**−2.09**	0.06	−0.11	0.48
	−0.71	−0.16	−0.74	−0.40	−0.05	−0.47	−0.96	−0.19	−0.44	0.46
	−0.86	−0.39	−0.78	0.07	−0.09	0.09	−1.27	−0.02	−0.27	0.43
S_{dDO}	−0.45	−0.22	−1.15	−0.21	−0.10	−0.03	−0.93	−0.10	−0.40	0.40
K_{DO_sed}	−0.38	−0.07	−0.14	−0.20	−0.04	−0.01	−0.58	0.03	−0.16	0.18
K_{DO_POM}	−0.38	−0.16	−0.52	−0.50	−0.05	−0.04	−0.82	−0.16	−0.12	0.31
fanB	−0.44	−0.13	−0.87	−0.04	−0.08	0.10	−1.10	−0.06	0.10	0.32
θ_{POM}	−0.38	−0.14	−0.54	−0.43	−0.07	0.01	−0.90	−0.13	−0.35	0.33
R_{POC}	−0.50	−0.16	−0.17	−0.12	−0.04	−0.06	−0.61	−0.01	−0.31	0.22
R_{POP}	−0.60	−0.39	1.20	0.08	0.05	0.09	0.30	0.05	−0.50	0.36
R_{PON}	0.43	0.37	−0.68	−0.10	−0.03	−0.11	−0.77	0.00	−0.64	0.35
D_{POM}	−0.96	−0.13	1.00	**−2.20**	−0.10	−0.02	−1.89	−0.15	**−3.56**	1.11
ρ_{POM}	**−2.11**	−0.34	**2.36**	**−4.73**	−0.26	−0.22	**−4.06**	−1.00	**−4.13**	**2.13**
KePOC	−0.59	−0.30	−0.71	0.05	−0.04	−0.05	−0.68	−0.08	−0.09	0.29
R_{DOP}	−0.60	−0.27	0.52	0.26	−0.09	0.04	−1.35	−0.03	0.00	0.35
R_{DON}	−0.58	−0.22	−0.95	−0.09	−0.07	0.00	−0.95	0.01	−0.02	0.32
KeDOC	−0.34	−0.10	0.18	−0.46	−0.04	−0.01	−0.77	0.05	0.00	0.22
θ_{N_2}	−0.53	−0.25	−0.74	0.43	−0.05	−0.07	−1.06	0.06	−0.25	0.38
R_{N_2}	−0.88	−0.58	−0.03	−0.03	−0.08	−0.09	−1.21	−0.03	0.01	0.33
K_{N_2}	−0.77	−0.56	0.16	−0.43	−0.08	−0.12	−1.16	−0.15	−0.05	0.39
θ_{NO}	−0.32	0.08	**−2.01**	−0.46	−0.06	−0.11	−0.51	−0.26	−0.21	0.45
R_{NO}	−0.91	−0.13	−0.09	0.10	−0.06	−0.10	−1.09	−0.09	−0.40	0.33
K_{NO}	−0.82	−0.28	**−2.03**	−0.08	−0.10	−0.04	−0.93	−0.30	−0.39	0.55
θ_{sed}	−0.38	−0.15	0.70	−0.26	−0.04	−0.11	−0.27	−0.07	−0.35	0.26
S_{dPO_4}	−0.34	−0.17	1.08	0.29	−0.12	−0.08	**−2.09**	0.06	−0.11	0.48
$K_{DO\_S_{dPO_4}}$	−0.71	−0.16	−0.74	−0.40	−0.05	−0.47	−0.96	−0.19	−0.44	0.46
S_{dNH_4}	−0.86	−0.39	−0.78	0.07	−0.09	0.09	−1.27	−0.02	−0.27	0.43
$K_{DO\_S_{dNH_4}}$	−0.45	−0.22	−1.15	−0.21	−0.10	−0.03	−0.93	−0.10	−0.40	0.40
>0.5%	34	2	66	34	7	6	74	8	31	28

Peri: *Peridinium*; Nano: nanoplankton; Aula: *Aulacoseira*; Pred: predatory zooplankton; Macro: macro-zooplankton; Micro: micro-zooplankton; Ave: average of absolute values.

grazing of phytoplankton by zooplankton; (3) grazing of POC by zooplankton; (4) contributions of excretion and mortality of phytoplankton to the POC pool; (5) contributions of egestion and mortality of zooplankton to the POC pool. The fluxes were calculated daily as a volumetrically integrated value over each of the DYRESM layers, and then averaged monthly. In Fig. 6, the primary productivity is expressed as a positive flux as it represents a source of carbon to the lake, while the other fluxes are expressed as negative, representing internal cycling of carbon (not sinks). Over the 24-month simulation period grazing of phytoplankton by zooplankton represented 4–105% of the monthly carbon assimilated in primary productivity (mean: 54%, S.D.: 30%) (Fig. 6). While grazing of POC was low (mean: 1%, S.D.: 2%)

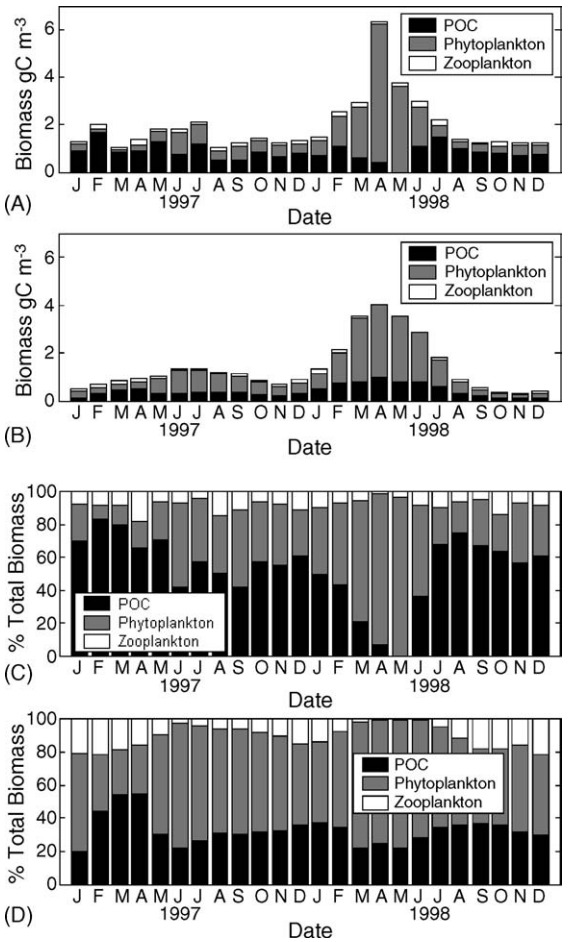

Fig. 5. Carbon biomass for field (A) and simulated (B) data and percentage of total biomass for field (C) and simulated (D) data presented as monthly averages for zooplankton, phytoplankton and detrital material.

during most of the year, the contribution increased significantly (9%) during the 1998 *Peridinium* bloom, when the contribution of phytoplankton to the detrital POC pool was also maximal. The simulated flux of carbon from phytoplankton and zooplankton to the POC pool ranged from 12 to 93% (mean: 34%) and from 1 to 23% (mean: 9%), respectively, of the carbon assimilated in primary productivity.

4.4. Nutrient dynamics

Four major phosphorus and nitrogen fluxes to and from the dissolved nutrient pools were extracted from

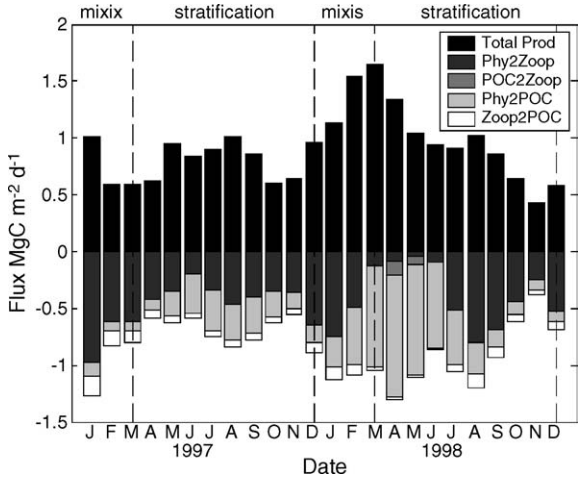

Fig. 6. Carbon fluxes ($g\,C\,m^{-2}\,day^{-1}$) for total primary productivity (Total Prod), grazing of phytoplankton (Phy2Zoop) and POC (POC2Zoop) by zooplankton and egestion and mortality of phytoplankton (Phy2POC) and zooplankton (Zoop2POC) to the POC pool. Corresponding periods of stratification and mixis are demarked by dashed lines.

the model in order to derive the contribution of zooplankton to the nutrient cycles of Lake Kinneret. These fluxes are shown in Fig. 7 and include: (1) phytoplankton uptake; (2) sediment–water exchange; (3) bacterially mediated mineralisation; (4) zooplankton excretion. A fifth component, external nutrient loading from inflows (5) (including dissolved inorganic and particulate species), was estimated from measured daily inflow volumes and nutrient concentrations. The fluxes are expressed as nutrient mass flux per day with respect to the whole lake. A negative flux (sink) represents loss of dissolved nutrients from the water column (e.g. phytoplankton uptake) and a positive flux (source) represents a gain (e.g. zooplankton excretion). The results, in Fig. 7A, show that although sediment exchange makes the greatest contribution to lake-wide phosphorus fluxes (range: 22–84%, mean: 54%), recycling via zooplankton excretion and bacterially mediated mineralisation also make significant contributions. Zooplankton excretion accounted for up to 46% of the phosphorus assimilated by phytoplankton (minimum: 3% (June 1998), maximum: 46% (August 1998), mean: 26%) and simulated values for bacterial mineralisation account for up to 33% of the phytoplankton demand (minimum: 4% (January 1998), max-

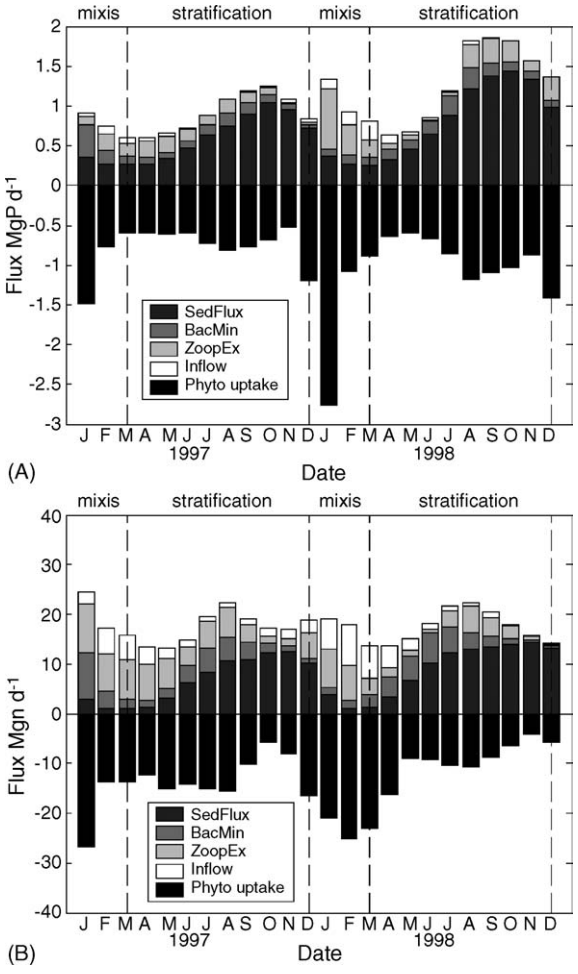

Fig. 7. (A) Phosphorus fluxes (g P m^{-2} day^{-1}) for total phytoplankton uptake (Phyto uptake), sediment flux (SedFlux), bacterially mediated mineralisation of POP to PO_4 (BacMin), zooplankton excretion (ZoopEx) and nutrient contribution from inflows (Inflow) and (B) nitrogen fluxes (g N m^{-2} day^{-1}) for total phytoplankton uptake (Phyto uptake), sediment flux (SedFlux), bacterially mediated mineralisation of PON to NH_4 (BacMin), zooplankton excretion (ZoopEx) and nutrient contribution from inflows (Inflow). Corresponding periods of stratification and mixis are demarked by dashed lines.

imum: 33% (June 1998), mean: 19%). For most of the year, the external phosphorus loading from inflows was small, contributing on average 6% to the phosphorus pool. However, during the months of February 1997 and January–March 1998, the inflow loading reached 11–27% of the total simulated flux from all sources, due to high discharge from the Jordan River inflow.

The patterns of external versus internal nutrient cycling were generally repeated in the simulation results for nitrogen fluxes (Fig. 7B). However, the contribution by sediment exchange as a fraction of the total sources of nitrogen was lower (range: 6–94%, mean: 43%). Also, zooplankton excretion as a percentage of phytoplankton uptake was higher, ranging from 5% (December 1998) to 58% (April 1997), with a mean of 32%. Simulated values for bacterial mineralisation accounted for up to 64% of the phytoplankton nitrogen uptake (minimum: 7% (January 1998), maximum: 64% (June 1998), mean: 25%). Again, external loading from inflows was low, averaging 15% of total sources but increasing to 47% during the high-flow periods.

Phosphorus fluxes from sediment release were low during mixis (early 1997) but gradually increased during the stratified period and then sharply declined again during mixis of early 1998. The sediment fluxes increased gradually during the stratified period of 1998 and peaked at a higher level than in 1997. This pattern was repeated with nitrogen release from the bottom sediments. The phosphorus flux from zooplankton excretion was high during mixis of early 1997 and then gradually decreased towards zero at the end of the stratified period. It was again high during early 1998 mixis before declining sharply with the onset of stratification in 1998. The flux from excretion increased in the middle of the 1998 stratified period, but declined again towards the end. This pattern was repeated in the nitrogen flux for zooplankton excretion.

5. Discussion

Quantitative model performance criteria with which to compare our results, though limited in number, suggest that our model performs relatively well in simulating the field data. For example, Ross et al. (1994) calculated NMAE values of 0.38, 1.16, 0.42, 0.63 and 0.65 for phytoplankton, DIN, zooplankton, carnivores and as an overall average, respectively, using a coupled hydrodynamic and ecological model of four fjords. On visual inspection, our model fit to measured data yielded a “generally good fit” compared with similar ecological models applied to data from Lake Ontario (Chen et al., 2002; Scavia, 1980), Lac de Pareloup

(Thébault and Salençon, 1993), Lake Zürich (Omlin et al., 2001) and Lake Burragorang (Romero et al., 2004).

The sensitivity analysis served two purposes, firstly to identify the parameters that required most attention to focus future modeling attempts and secondly to identify which variables are most sensitive to changes in parameters. The predatory zooplankton and macro-zooplankton parameters (found to be the most sensitive) were estimated from experimental data on the main species of zooplankton from each group, isolated from Lake Kinneret. Future experimental studies should focus on expanding the experiments to other species to establish parameters representative to the groups. The other significant parameter was the density of POM. Since availability of inorganic nutrients is dependent on the mineralisation of POM, it would be expected that loss of POM through settling will affect all levels of the trophic food web. Although this analysis does not claim to answer questions on the bottom-up/top-down control debate, it is interesting to note that the most sensitive parameters related to both top-down (zooplankton predation) and bottom up (relating to the supply of nutrients to the photic zone) control. In contrast, Omlin et al. (2001) found that parameters related to growth, respiration and death of both phytoplankton and zooplankton contributed the greatest uncertainty to model results and Chen et al. (2002) found that the most sensitive parameters in their model related to phytoplankton growth rate and nutrient limitation. The most sensitive variables were PO_4, predatory zooplankton and *Peridinium*. Again, PO_4 and predatory zooplankton come from the opposite sides of the bottom-up/top-down control. It is possible that the *Peridinium* showed high sensitivity due to the fact that during most of the simulation period it is the dominant plankton group in terms of carbon biomass.

Our simulation results produced an estimate of over 50% of primary production transferred via zooplankton grazing to secondary production. To place our research in context with other studies, we compared our simulated estimates of the percentage of primary production transferred via zooplankton grazing to secondary production. In a seasonal mass balance model of Lake Kinneret using data from 1989 to 1992, Hart et al. (2000) estimated, on average, that 42% of primary production was consumed directly by zooplankton. Our estimate of 54% is higher but may be explained by the lower *Peridinium* biomass in 1997. A lower *Peridinium* biomass in the bloom phase means that a greater percentage of primary productivity is partitioned into the highly grazed nanoplankton component. In other systems, Lin et al. (1999) estimated that 58% of primary production was transferred to secondary producers based on a simple mass balance for a sandy barrier lagoon in southwestern Taiwan, Laws et al. (1988) used measurements from a field study to calculate a transfer of 50% in Auke Bay, Alaska, and Scavia (1980) used an NPZ model similar to ours to estimate 62% transfer efficiency of carbon in Lake Ontario. Although there is uncertainty in estimates of the percentage of primary production transferred to secondary producers, relatively large values are widespread across different systems, even with different methods of analysis. Thus, as transfer of primary production to higher trophic levels via secondary production is highly important, accurately simulating and understanding trophic dynamics in these systems will clearly be reliant on quantifying the role of secondary production.

A field study of the contribution of zooplankton to nutrient fluxes in Lake Biwa, Japan, found that, on average, the fraction of nitrogen regenerated by zooplankton during stratification was 50% of that fixed by primary production, compared to 15% for phosphorus (Urabe et al., 1995). In contrast, we estimate 32 and 26% for nitrogen and phosphorus, respectively. Urabe et al. (1995) attributed the lower relative contribution of zooplankton to the phosphorus pool to phosphorus limitation. In our study, the average simulated N:P ratio of the nanoplankton for 1997–1998 was 13.5 (w/w), the N:P ratio of macro-zooplankton the main grazer was set at 7.5 and the average simulated N:P ratio of zooplankton excretion was 21. This suggests that for Lake Kinneret the nanoplankton are P-limited and zooplankton growth may also be strongly influenced by P. The main reason the values of excretion expressed as a percentage of phytoplankton uptake do not differ widely is due to the fact that mixing from P released from the bottom sediments gives a proportionately greater contribution to available nutrients in the photic zone than for nitrogen. On this basis we would conclude that the effect of zooplankton grazing and excretion of nitrogen and phosphorus does not appear to significantly alter the elemental balance in the photic zone.

6. Conclusion

The model used here was shown to reproduce the seasonal variation of biomass of the dominant phytoplankton and zooplankton in Lake Kinneret. The model produced the best results when variability in field data was low and showed the biggest divergence when there was large scatter in the field data. The model results showed that even though zooplankton biomass at no stage exceeded more than 22% of the total plankton carbon, zooplankton excretion of dissolved nutrients can account for up to 52 and 48% of the phytoplankton demand for phosphorus and nitrogen, respectively. Using the model output, we were able to compare the hydrodynamic and ecological sources and sinks of nutrients in the photic zone to determine which integrating factors ultimately determine seasonal patterns in plankton ecology. The ability of numerical models, such as the one used in this study, to couple ecological and physical variables enables researchers to ask questions that relate to the integration of both biotic and abiotic factors in limnological nutrient cycles. Further improvements to the current model formulation will enable us to extend the ecosystem focus to questions such as the role of micro-zooplankton in nutrient recycling.

Acknowledgements

The authors thank the following organisations for providing the data used in this study: Mekorot Watershed Unit, Israel Hydrological Services, Israel Meteorological Services, the Kinneret Authority, Israeli Water Commission (IWC) and the Kinneret Limnological Laboratory (KLL). We particularly thank Ami Nishri, Yossi Yacobi and Arkadi Parparov for providing unpublished data and advice, Anas Ghadouani for his valuable comments on the manuscript and the Contract Research Group at the Centre for Water Research (CWR), in particular David Horn, for technical support for the project. Funding was provided by the IWC via the Kinneret Modeling Project, conducted jointly by KLL and CWR. The first author was further funded by an Australian Postgraduate (Industry) scholarship, sponsored by the Wheatbelt Development Commission.

References

Alewell, C., Manderscheid, B., 1998. Use of objective criteria for the assessment of biogeochemical ecosystem models. Ecol. Model. 107, 213–224.

Andersen, T., Hessen, D.O., 1991. Carbon, nitrogen, and phosphorus content of freshwater zooplankton. Limnol. Oceanogr. 36, 807–814.

Blumenshine, S.C., Hambright, K.D., 2003. Top-down control in pelagic systems: a role for invertebrate predation. Hydrobiologia 491, 347–356.

Carlotti, F., Günther, R., 1996. Seasonal dynamics of phytoplankton and *Calanus finmarchicus* in the North Sea as revealed by a coupled one-dimensional model. Limnol. Oceanogr. 41, 522–539.

Carpenter, S.R., Kitchell, J.F., 1993. Simulation models of the trophic cascade: predictions and evaluations. In: Kitchell, S.C.J. (Ed.), The Trophic Cascade in Lakes. Cambridge University Press.

Chen, C., et al., 2002. A model study of the coupled biological and physical dynamics of Lake Michigan. Ecol. Model. 152, 145–168.

Cole, J.F., Jones, R.C., 2000. Effect of temperature on photosynthesis–light response and growth of four phytoplankton species isolated from a tidal freshwater river. J. Phycol. 36, 7–16.

Cole, J.J., Carpenter, S.R., Kitchell, J.F., Pace, M.L., 2002. Pathways of organic carbon utilization in small lakes: results from a whole-lake 13C addition and coupled model. Limnol. Oceanogr. 47, 1664–1675.

Easton, J., Gophen, M., 2003. Diel variation in the vertical distribution of fish and plankton in Lake Kinneret: a 24-h study of ecological overlap. Hydrobiologia 491, 91–100.

Gal, G., Imberger, J., Zohary, T., Antenucci, J.P., Anis, A., Rosenberg, T., 2003. Simulating the thermal dynamics of Lake Kinneret. Ecol. Model. 162, 69–86.

Gilbert, P.M., 1998. Interactions of top-down and bottom-up control in planktonic nitrogen cycling. Hydrobiologia 363, 1–12.

Gophen, M., 1976a. Temperature dependence of food intake, ammonia excretion and respiration in *Ceriodaphnia reticulata* (Jurine) (Lake Kinneret, Israel). Freshwater Biol. 6, 451–455.

Gophen, M., 1976b. Temperature effect on lifespan, metabolism and development time of *Mesocyclops leuckarti* (Claus). Oceologia 25, 271–277.

Gophen, M., 1984. The impact of zooplankton status on the management of Lake Kinneret (Israel). Hydrobiologia 113, 249–258.

Gophen, M., Azoulay, B., 2002. The trophic status of zooplankton communities in Lake Kinneret (Israel). Verh. Int. Ver. Limnol. 28, 836–839.

Griffin, S.L., Herzfeld, M., Hamilton, D.P., 2000. Modelling the impact of zooplankton grazing on phytoplankton biomass during a dinoflagellate bloom in the Swan River estuary, Western Australia. Ecol. Eng. 16, 373–394.

Hadas, O., Berman, T., 1998. Seasonal abundance and vertical distribution of protozoa (flagellates, ciliates) and bacteria in Lake Kinneret, Israel. Aquat. Microbiol. 14, 161–170.

Håkanson, L., Boulion, V.V., 2003. Modelling production and biomasses of herbivorous and predatory zooplankton in lakes. Ecol. Model. 161, 1–33.

Hambright, K.D., Gophen, M., Serruya, S., 1994. Influence of long-term climatic changes on the stratification of a subtropical, warm monomictic lake. Limnol. Oceanogr. 39, 1233–1242.

Haney, J.F., Trout, M.A., 1985. Selective grazing by zooplankton in Lake Titicaca. Ergeb. Limnol. 21, 147–160.

Hart, D.R., Stone, L., Berman, T., 2000. Seasonal dynamics of the Lake Kinneret food web: the importance of the microbial loop. Limnol. Oceanogr. 45, 350–361.

Hongping, P., Jianyi, M., 2002. Study on the algal dynamic model for West Lake Hangzhou. Ecol. Model. 148, 67–77.

Hudson, J.J., Taylor, W.D., 1996. Measuring regeneration of dissolved phosphorus in planktonic communities. Limnol. Oceanogr. 41, 1560–1565.

Hudson, J.J., Taylor, W.D., Schindler, D.W., 1999. Planktonic nutrient regeneration and cycling efficiency in temperate lakes. Nature 400, 659–661.

Ji, R., et al., 2005. Influences of suspended sediments on the ecosystem in Lake Michigan: a 3-D coupled bio-physical modeling experiment. Ecol. Model. 152, 169–190.

Jewson, D.H., 1977. Light penetration in relation to phytoplankton content of the eutrophic zone of Lough Neagh, N. Ireland. Oikos 28, 74–83.

Jorgensen, S.E., Bendoricchio, G., 2001. Fundamentals of Ecological Modeling, third ed. Elsevier.

Kirk, J.T.O., 1994. Light and Photosynthesis in Aquatic Ecosystems, second ed. Cambridge Press.

Krivtsov, V., Goldspink, C., Sigee, D.C., Bellinger, E.G., 2001. Expansion of the model 'Rostherne' for fish and zooplankton: role of top-down effects in modifying the prevailing pattern of ecosystem functioning. Ecol. Model. 138, 153–171.

Landry, M.R., Hassett, R.P., 1985. Time scales in behavioral, biochemical, and energetic adaptations to food-limiting conditions by a marine copepod. Ergeb. Limnol. 21, 209–222.

Laws, E.A., Bienfang, P.K., Ziemann, D.A., Conquest, L.D., 1988. Phytoplankton population dynamics and the fate of production during the spring bloom in Auke Bay, Alaska. Limnol. Oceanogr. 33, 57–65.

Lehman, J.T., 1980. Release and cycling of nutrients between planktonic algae and herbivores. Limnol. Oceanogr. 25, 620–632.

Lin, H.J., et al., 1999. A trophic model of a sandy barrier lagoon at Chiku in southwestern Taiwan. Estuarine Coastal Shelf Sci. 58, 575–588.

Lunte, C.C., Leucke, C., 1990. Trophic interactions of Leptodora in Lake Mendota. Limnol. Oceanogr. 35, 1091–1100.

Madoni, P., Berman, T., Hadas, O., Pinkas, R., 1990. Food selection and growth of the planktonic ciliate *Coleps hirtus* isolated from a monomictic subtropical lake. J. Plankton Res. 12, 735–741.

Mehner, T., 2000. Influence of spring warming on the predation rate of underyearling fish on Daphnia—a deterministic simulation approach. Freshwater Biol. 45, 253–263.

Omlin, M., Reichert, P., Forster, R., 2001. Biogeochemical model of Lake Zürich: model equations and results. Ecol. Model. 141, 77–103.

Osidele, O.O., Beck, M.B., 2004. Food web modelling for investigating ecosystem behaviour in large reservoirs of the south-eastern United States: lessons from Lake Lanier Georgia. Ecol. Model. 173, 129–158.

Pollingher, U., 1986. Phytoplankton periodicity in a subtropical lake (Lake Kinneret, Israel). Hydrobiologia 138, 127–138.

Pollingher, U., Berman, T., 1982. Relative contributions of net and nano phytoplankton to primary production in Lake Kinneret (Israel). Arch. Hydrobiol. 96, 33–46.

Putt, M., Stockner, 1989. An experimentally determined carbon:volume ratio for marine oligotrichous ciliates from estuarine and coastal waters. Limnol. Oceanogr. 34, 1097–1103.

Reynolds, C.S., 1984. The Ecology of Freshwater Phytoplankton. Cambridge Press.

Robson, B.J., Hamilton, D.P., 2004. Three-dimensional modelling of a Microcystis bloom event in the Swan River estuary, Western Australia. Ecol. Model. 174, 203–222.

Romero, J.R., Antenucci, J.P., Imberger, J., 2004. One- and three-dimensional biogeochemical simulations of two differing reservoirs. Ecol. Model. 174, 143–160.

Ross, A.H., Gurney, S.C., Heath, M.R., 1994. A comparative study of the ecosystem dynamics of four fjords. Limnol. Oceanogr. 39, 318–343.

Rukhovets, L.A., Astrakhantsev, G.P., Menshutkin, V.V., Minina, T.R., Petrova, N.A., Poloskov, V.N., 2003. Development of Lake Ladoga ecosystem models: modeling of the phytoplankton succession in the eutrophication process. I. Ecol. Model. 165, 49–77.

Scavia, D., 1980. An ecological model of Lake Ontario. Ecol. Model. 8, 49–78.

Scavia, D., Lang, G.A., Kitchell, J.F., 1988. Dynamics of Lake Michigan plankton: a model evaluation of nutrient loading, competition and predation. Can. J. Fish. Aquat. Sci. 45, 165–177.

Serruya, C., 1978. Lake Kinneret. Junk.

Serruya, C., Berman, T., 1976. Phosphorus, nitrogen and the growth of algae in Lake Kinneret. J. Phycol. 11, 155–162.

Serruya, C., Edelstein, M., Pollingher, U., Serruya, S., 1974. Lake Kinneret sediments: nutrient composition of the pore water and mud water exchanges. Limnol. Oceanogr. 19, 489–508.

Stemberger, R.S., Gilbert, J.J., 1985. Assessment of threshold food levels and population growth in planktonic rotifers. Ergeb. Limnol. 21, 269–276.

Sterner, R.W., 1986. Herbivores' direct and indirect effects on algal populations. Science 231, 605–607.

Thébault, J., Salençon, M., 1993. Simulation model of a mesotrophic reservoir (Lac de Pareloup, France): biological model. Ecol. Model. 65, 1–30.

Urabe, J., Nakanishi, M., Kawabata, K., 1995. Contribution of metazoan plankton to the cycling of nitrogen and phosphorus in Lake Biwa. Limnol. Oceanogr. 40, 232–241.

Vanni, M.J., 2002. Nutrient cycling by animals in freshwater ecosystems. Annu. Rev. Ecol. Syst. 33, 341–370.

Wen, Y.H., Peters, R.H., 1994. Empirical models of phosphorus and nitrogen excretion rates by zooplankton. Limnol. Oceanogr. 39, 1669–1679.

Wynne, D., Panti, N.J., Aaronson, S., Berman, T., 1982. The relationship between nutrient status and chemical composition of *Peridinium cinctum* during the bloom of Lake Kinneret. J. Plankton Res. 4, 125–134.

Yacobi, Y.Z., Kalikhman, I., Gophen, M., Walline, P., 1993. The spatial distribution of temperature, oxygen, plankton and fish determined simultaneously in Lake Kinneret, Israel. J. Plankton Res. 15, 589–601.

Yeates, P.S., Imberger, J., 2004. Pseudo two-dimensional simulations of internal and boundary fluxes in stratified lakes and reservoirs. Int. J. River Basin Res. 1, 1–23.

Zohary, T., 2004. Changes to the phytoplankton assemblage of Lake Kinneret after decades of a predictable, repetitive pattern. Freshwater Biol. 49, 1355–1371.

Zohary, T., Erez, J.G.M., Bernam-Frank, I., Stiller, M., 1994. Seasonality of stable carbon isotopes within the pelagic food web of Lake Kinneret. Limnol. Oceanogr. 39, 1030–1043.